

PL-TR-96-2283

SSS-DTR-96-15583

## Investigations of Regional Phase Spectral Ratios: Transportability and Measurement Algorithms

Theron J. Bennett  
Margaret E. Marshall  
Brian W. Barker  
John R. Murphy

Maxwell Technologies, Inc.  
8888 Balboa Ave.  
San Diego, CA 92123-1506

October, 1996

19970331 096

Scientific Report No. 1

DTIC QUALITY INSPECTED 4

Approved for public release; distribution unlimited




**PHILLIPS LABORATORY**  
**Directorate of Geophysics**  
**AIR FORCE MATERIEL COMMAND**  
**HANSCOM AIR FORCE BASE, MA 01731-3010**

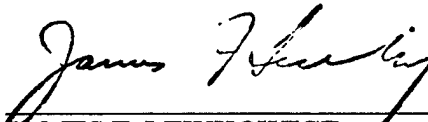
SPONSORED BY  
Air Force Technical Applications Center  
Directorate of Nuclear Treaty Monitoring  
Project Authorization T/5101

MONITORED BY  
Phillips Laboratory  
CONTRACT No. F19628-95-C-0108

The views and conclusions contained in this document are those of the authors and should not be interpreted as representing the official policies, either express or implied, of the Air Force or U.S. Government.

This technical report has been reviewed and is approved for publication.

  
DELAINE R. REITER  
Contract Manager  
Earth Sciences Division

  
JAMES F. LEWKOWICZ  
Director  
Earth Sciences Division

This report has been reviewed by the ESD Public Affairs Office (PA) and is releasable to the National Technical Information Service (NTIS).

Qualified requestors may obtain copies from the Defense Technical Information Center. All others should apply to the National Technical Information Service.

If your address has changed, or you wish to be removed from the mailing list, or if the addressee is no longer employed by your organization, please notify PL/IM, 29 Randolph Road, Hanscom AFB, MA 01731-3010. This will assist us in maintaining a current mailing list.

Do not return copies of this report unless contractual obligations or notices on a specific document requires that it be returned.

# REPORT DOCUMENTATION PAGE

*Form Approved*  
OMB No. 0704-0188

Public reporting burden for this collection of information is estimated to average 1 hour per response, including the time for reviewing instructions, searching existing data sources, gathering and maintaining the data needed, and completing and reviewing the collection of information. Send comments regarding this burden estimate or any other aspect of this collection of information, including suggestions for reducing this burden, to Washington Headquarters Services, Directorate for Information Operations and Reports, 1215 Jefferson Davis Highway, Suite 1204, Arlington, VA 22202-4302, and to the Office of Management and Budget, Paperwork Reduction Project (0704-0188), Washington, DC 20503.

1. AGENCY USE ONLY <i>(Leave blank)</i>	2. REPORT DATE October, 1996	3. REPORT TYPE AND DATES COVERED Scientific No. 1	
4. TITLE AND SUBTITLE INVESTIGATIONS OF REGIONAL PHASE SPECTRAL RATIOS: TRANSPORTABILITY AND MEASUREMENT ALGORITHMS		5. FUNDING NUMBERS F19628-95-C-0108 PE 35999F PR 5101 TA GM WU AD	
6. AUTHOR(S) Theron J. Bennett, Margaret E. Marshall, Brian W. Barker, and John R. Murphy		8. PERFORMING ORGANIZATION REPORT NUMBER SSS-DTR-96-15583	
7. PERFORMING ORGANIZATION NAME(S) AND ADDRESS(ES) Maxwell Technologies, Inc. 8888 Balboa Avenue San Diego, CA 92123-1506		10. SPONSORING/MONITORING AGENCY REPORT NUMBER PL-TR-96-2283	
9. SPONSORING/MONITORING AGENCY NAME(S) AND ADDRESS(ES) Phillips Laboratory 29 Randolph Road Hanscom AFB, MA 01731-3010 Contract Manager: Delaine Reiter/GPE		11. SUPPLEMENTARY NOTES	
12a. DISTRIBUTION/AVAILABILITY STATEMENT Approved for public release; distribution unlimited		12b. DISTRIBUTION CODE	
13. ABSTRACT <i>(Maximum 200 words)</i> Use of regional phase spectral ratios as discriminants involves parameterization of differences in the relative spectral shape of regional phase signals from different source types. This research program has been directed at improved understanding of the influences of source excitation and propagation on the transportability of regional phase spectral ratio discriminants. For use in these investigations, high-quality digital waveform data from regional seismic stations have been compiled for underground nuclear explosions and comparable earthquakes in the western U.S. and Eurasia. We have used some simple bandpass filter algorithms to extract consistent signal spectra and spectral ratios for group velocity windows associated with individual regional phases. Effects of source size and group velocity windows have been analyzed for selected event samples. In the western U.S. our observations indicate L <sub>g</sub> and P <sub>g</sub> spectral ratio differences between nuclear explosions and earthquakes; but these are diminished when source size differences are taken into account. Similar measurements for Eurasian events show only small differences between source types; and, if source scaling is applied, trends in the spectral ratios for explosions and earthquakes may be opposite to those seen in the western U.S.			
14. SUBJECT TERMS Seismic                      Regional                      Europe                      Spectra Discrimination      North America      Asia                      Transportability			15. NUMBER OF PAGES 72
17. SECURITY CLASSIFICATION OF REPORT UNCLASSIFIED			16. PRICE CODE
18. SECURITY CLASSIFICATION OF THIS PAGE UNCLASSIFIED	19. SECURITY CLASSIFICATION OF ABSTRACT UNCLASSIFIED	20. LIMITATION OF ABSTRACT UNLIMITED	

## Table of Contents

	<u>Page</u>
1. Introduction.....	1
1.1 Objectives.....	1
1.2 Accomplishments.....	2
1.3 Report Organization.....	3
2. Regional Discrimination Database.....	4
2.1 Availability of Digital Data for Discrimination Studies.....	4
2.2 Western U.S. Event and Station Locations.....	5
2.3 Eurasian Event and Station Locations.....	10
2.4 Regional Event Magnitudes.....	14
3. Further Analysis of Western U.S. Data.....	18
3.1 Previous Findings.....	18
3.2 Analysis Procedures.....	18
3.3 Application to Western U.S. Event Samples.....	26
3.4 Effects of Source Size on Regional Phase Spectra.....	29
4. Analyses of Asian Data.....	35
4.1 Previous Findings.....	35
4.2 Application of Analysis Techniques to WMQ Records.....	36
4.3 Application of Analyses to New Data from Soviet PNE's.....	45
5. Summary and Conclusions.....	54
5.1 Review of Procedures.....	54
5.2 Summary of Main Findings.....	55
5.3 Plans for Future Work.....	56
6. References.....	58

## List of Illustrations

	<u>Page</u>
1 Map of western U.S. showing location of NTS relative to regional stations with good digital data which are currently in the database	6
2 Distances of observations for selected NTS nuclear explosions and stations providing good digital waveforms at regional distances which are currently in the database.....	7
3 Distances of observations for selected western U.S. earthquakes and stations providing good digital waveforms at regional distances which are currently in the database.....	8
4 Map of Eurasia showing location of principal nuclear test sites relative to regional stations with good digital data which are currently in the database.....	11
5 Distances of observations for selected Asian nuclear explosions and stations providing good digital waveforms at regional distances which are currently in the database.....	12
6 Distances of observations for selected Eurasian earthquakes and stations providing good digital waveforms at regional distances which are currently in the database.....	13
7(a) Distribution of western U.S. nuclear test observations in regional database with respect to event magnitude.....	15
7(b) Distribution of western U.S. earthquake observations in regional database with respect to event magnitude.....	15
8(a) Distribution of Eurasian nuclear test observations in regional database with respect to event magnitude.....	16
8(b) Distribution of Eurasian earthquake observations in regional database with respect to event magnitude.....	16
9 Map showing the locations of NTS nuclear explosions and nearby earthquakes relative to the LLNL network stations.....	20
10 Traditional bandpass filter analysis of NTS explosion GORBEA recorded at station KNB.....	21
11 Traditional bandpass filter analysis of May 12, 1982 earthquake near NTS recorded at station KNB.....	23

12	Comparison of $L_g$ spectral estimates at station KNB for broad traditional bandpass filters and narrow Gaussian filters for nuclear test GORBEA and 05/12/82 earthquake.....	25
13	Relative $L_g$ spectral estimates obtained for NTS nuclear tests and nearby earthquakes from traditional bandpass filter analyses of records at station KNB.....	27
14	Relative $L_g$ spectral estimates obtained for NTS nuclear tests and nearby earthquakes from traditional bandpass filter analyses of records at station MNV.....	28
15	Comparison of average $L_g$ spectral estimates at station KNB for 5 NTS nuclear tests, 5 nearby earthquakes, and 5 scaled NTS nuclear tests.....	31
16	Comparison of average $P_g$ spectral estimates at station KNB for 5 NTS nuclear tests, 5 nearby earthquakes, and 5 scaled NTS nuclear tests.....	33
17	Map showing the locations of Soviet nuclear explosions and nearby earthquakes relative to station WMQ in China.....	38
18	Relative $L_g$ spectral estimates obtained for Shagan River nuclear explosions from traditional bandpass filter analyses of records at station WMQ using amplitudes measured in windows from 3.6 km/sec to 3 km/sec.....	39
19	Relative $L_g$ spectral estimates obtained for Shagan River nuclear explosions from traditional bandpass filter analyses of records at station WMQ using amplitudes measured in windows from 4.6 km/sec to 3 km/sec.....	41
20	Relative $L_g$ spectral estimates obtained for Asian earthquakes from traditional bandpass filter analyses of records at station WMQ at similar epicentral distances to the nuclear explosions at WMQ for measurements in window from 3.6 km/sec to 3 km/sec.....	42
21	Relative $L_g$ spectral estimates obtained for Asian earthquakes from traditional bandpass filter analyses of records at station WMQ at similar epicentral distances to the nuclear explosions at WMQ for measurements in window from 4.6 km/sec to 3 km/sec.....	43
22	Comparison of average $L_g$ spectral estimates for 5 Shagan River nuclear explosions recorded at station WMQ with average $L_g$ spectral for 3 earthquakes to the south-southwest and for 2 earthquakes to the south at similar epicentral distances.....	44

23	Map showing the locations of selected Soviet PNE explosions relative to station BRV.....	46
24	Traditional bandpass filter analysis of Soviet PNE explosion of December 10, 1980 recorded at station BRV (R = 980 km) .....	48
25	Traditional bandpass filter analysis of Soviet PNE explosion of October 26, 1980 recorded at station BRV (R = 925 km).....	49
26	Relative $L_g$ spectral estimates obtained for PNE explosions from traditional bandpass filter analyses of records at station BRV using amplitudes measured in window from 3.6 km/sec to 3 km/sec.....	50
27	Relative $L_g$ spectral estimates obtained for PNE explosions from traditional bandpass filter analyses of records at station BRV using amplitudes measured in window from 3.6 km/sec to 3 km/sec after adjustment for BRV instrument response.....	52

# 1. Introduction

## 1.1 Objectives

Under a Comprehensive Test Ban Treaty (CTBT), regional seismic stations are expected to play a key role in monitoring at the low thresholds of interest. For small events regional stations are likely to provide the only seismic signals with adequate strength above the background noise to use for event detection, location, and discrimination. Since the status of regional seismic discrimination was reviewed by Blandford (1981) and Pomeroy et al. (1982), considerable progress has been made in understanding the effects of seismic source mechanisms on regional phase excitation and the influences of geologic structure on regional phase propagation. However, many problems remain with regard to determining how potential regional discriminants will perform in uncalibrated regions, as would be required in the context of a CTBT.

This research project is focused on a particular class of regional discriminants, viz. those associated with frequency differences in the signals from different source types. In particular, regional phase spectral ratios involve exploitation and parameterization of differences in the relative spectral shape, or frequency content, of regional phase signals from different source types. The principal objectives of this research program are to develop more complete understanding of the influences of source excitation and propagation on the transportability of regional phase spectral ratio discriminants and to define criteria for application of spectral ratio discrimination methods in uncalibrated areas. We anticipate that, by applying appropriate corrections for source and propagation effects, we will be able to more reliably discern source-dependent differences in the regional phase spectral ratios which should be transportable into different, uncalibrated monitoring environments.

## 1.2 Accomplishments

To accomplish our research objectives, we have sought to collect regional waveform data from a variety of source types including nuclear explosions, earthquakes, rockbursts, and chemical blasts for a range of propagation environments. Although nuclear explosions provide the only true test of regional discrimination techniques, regional waveform data for nuclear tests are limited to observations from only a few source regions. We have assembled a representative database of regional recordings for nuclear explosions from the primary test areas at the Nevada Test Site (NTS), the former Soviet test site at Shagan River (SR) in East Kazakhstan, the former Soviet test site at Novaya Zemlya (NZ), and the Chinese test site at Lop Nor. For comparisons we have also collected regional data, recorded in many cases at the same stations, from other seismic source types in the same or nearby regions; and we are continuing to supplement this database with additional events recorded at the modern IDC and other digital stations for areas of interest.

In our investigations we have been focusing initially on the spectral behavior of the regional phases from these sources in the various regions. We have applied some alternative systematic spectral measurement schemes and confirmed the differences in spectral behavior of the regional phases  $P_g$  and  $L_g$  for NTS explosions and nearby earthquakes, which had been found several years ago. The same measurements on Asian events do not show similar behavior for the different source types and may, in fact, show opposite trends.

To extend discrimination capabilities between regions and to permit more appropriate comparisons between events at different regional distances, procedures are being developed to account for propagation differences. The relative spectral content of regional seismic signals can also be affected by

source size, so discriminant measures should also be adjusted for magnitude differences between events. We have identified scaling procedures which enable spectral adjustments for source size, and we have been seeking to determine attenuation relations for various regions and phases which will permit corrections for propagation.

### **1.3 Report Organization**

This report is divided into five sections including these introductory remarks. Section 2 describes the event database which we have been working with. Section 3 discusses the spectral measurement procedures applied to the western U.S. database and reconsiders the regional phase spectral differences with appropriate scaling adjustments for differences in source size. Section 4 describes the same procedures applied to the data from Asian events. Section 5 summarizes the preliminary results and describes the plan for continuing work to evaluate the spectral ratio discriminants.

## **2. Regional Discrimination Database**

### **2.1 Availability of Digital Data for Discrimination Studies**

Regional recordings of underground nuclear explosions cover a very limited domain in space and time. All but a few U.S. underground nuclear tests were conducted at NTS in the western U.S. The majority of nuclear tests by the former Soviet Union were conducted at their test site in East Kazakhstan; although they have also conducted numerous tests at Novaya Zemlya (NZ), and in the North Caspian basin, as well as a series of Peaceful Nuclear Explosions (PNE) over a large geographical region. The Chinese have conducted nuclear explosions at Lop Nor in western China, and the Indian government has conducted nuclear weapons tests at a site in that country. France has conducted nuclear explosion tests in northern Africa and in the South Pacific. So, while there have been underground nuclear explosions in a variety of regions around the world, there are large portions of the world where there is little or no experience with nuclear tests.

A second factor affecting availability of data for regional discrimination studies is the history of seismic monitoring. Limited historic data from the past has been overwhelmed in recent years by the onslaught of digital seismic data from high-quality single stations and arrays. Although these new data include many interesting seismic events, they include very few nuclear explosion recordings because of testing moratoria and the tapering off of the nuclear testing programs in most countries. The new data alone are inadequate to calibrate regional discrimination capabilities. Fortunately, we do have historical regional data from many of the nuclear tests in some areas, which can be useful in helping to infer the characteristics of regional signals from potential nuclear tests in uncalibrated regions. The best inferences are likely to come from combining knowledge of regional propagation for earthquakes gained from the

new monitoring efforts with knowledge of nuclear explosion-vs-earthquake excitation differences gained from the historical database.

## **2.2 Western U.S. Event and Station Locations**

The best controlled data sample for developing an understanding of the differences between nuclear explosions and earthquakes in excitation of regional signals is the large body of regional recordings from NTS nuclear explosions and nearby earthquakes. These data formed the basis for the original  $L_g$  spectral ratio as a discriminant (cf. Murphy and Bennett, 1982). In the course of past studies and the current research program, we have collected digital waveform data from selected NTS nuclear explosions and earthquakes in the surrounding regions. The regional stations (cf. Figure 1) for which we have data from this region include the Lawrence Livermore National Laboratory (LLNL) network stations (viz. MNV, KNB, LAC, and ELK), the old VELA array stations (viz. TFO, UBO, and BMO), the SRO station ANMO, and the RSTN station RSSD. At each of these stations we have regional digital data available from several NTS nuclear explosion tests and earthquakes from the surrounding region. We also currently have limited data from a few NTS explosions and nearby earthquakes recorded at the Texas array station (viz. TXAR) at Lajitas, Texas. Regional data from western U.S. seismic events are also available for several other regional and far-regional stations. In general, the regional signals at the nearer western U.S. stations are good and could be useful for more detailed analyses; however, signal-to-noise levels are poor at the farther stations, especially for  $L_g$ .

Figure 2 shows the distribution with respect to epicentral distance of the western U.S. nuclear explosions currently in our database, and Figure 3 shows a similar distribution for western U.S. earthquakes. For NTS explosions the

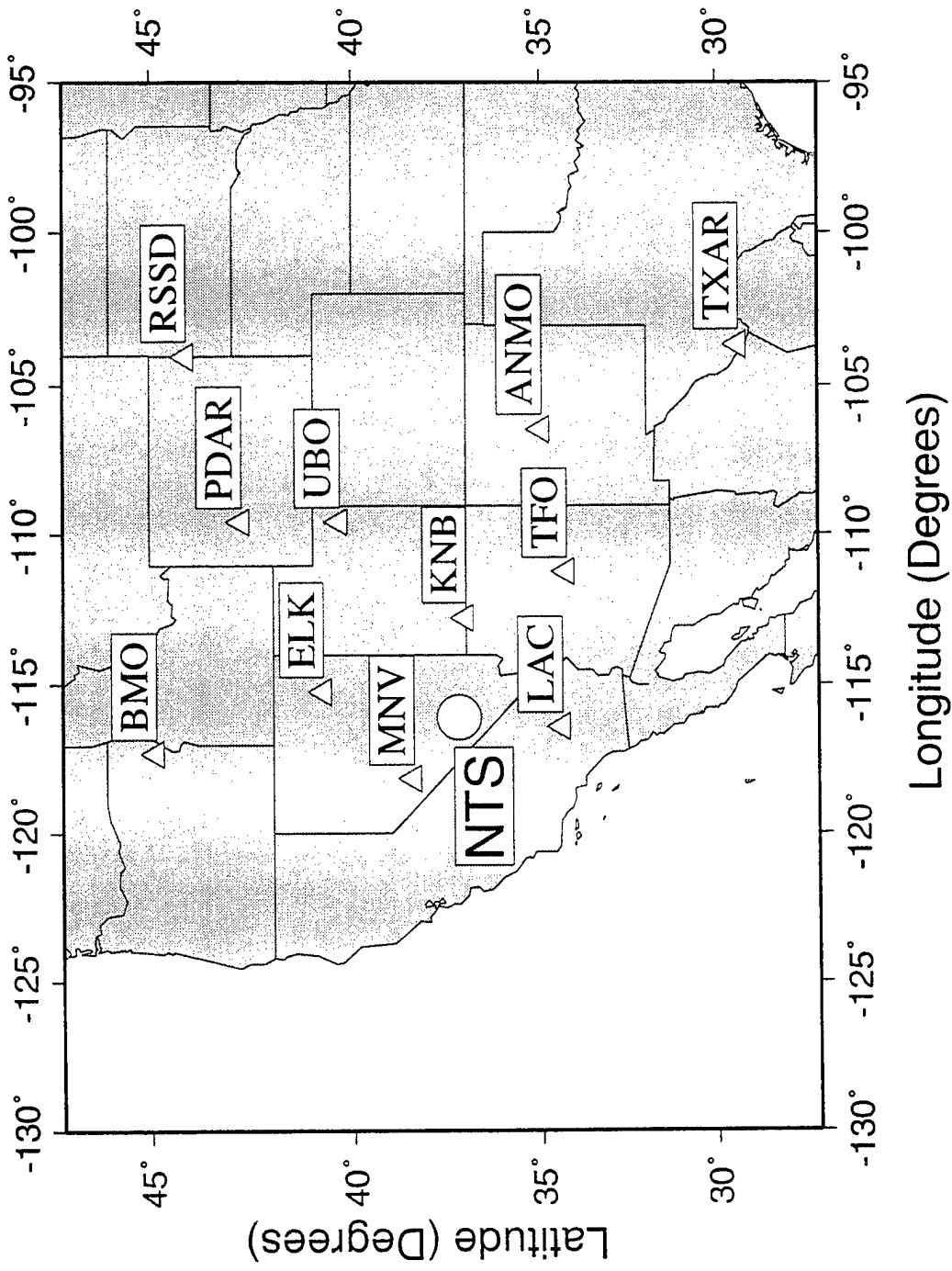


Figure 1. Map of western U.S. showing location of NTS relative to regional stations with good digital data which are currently in the database.

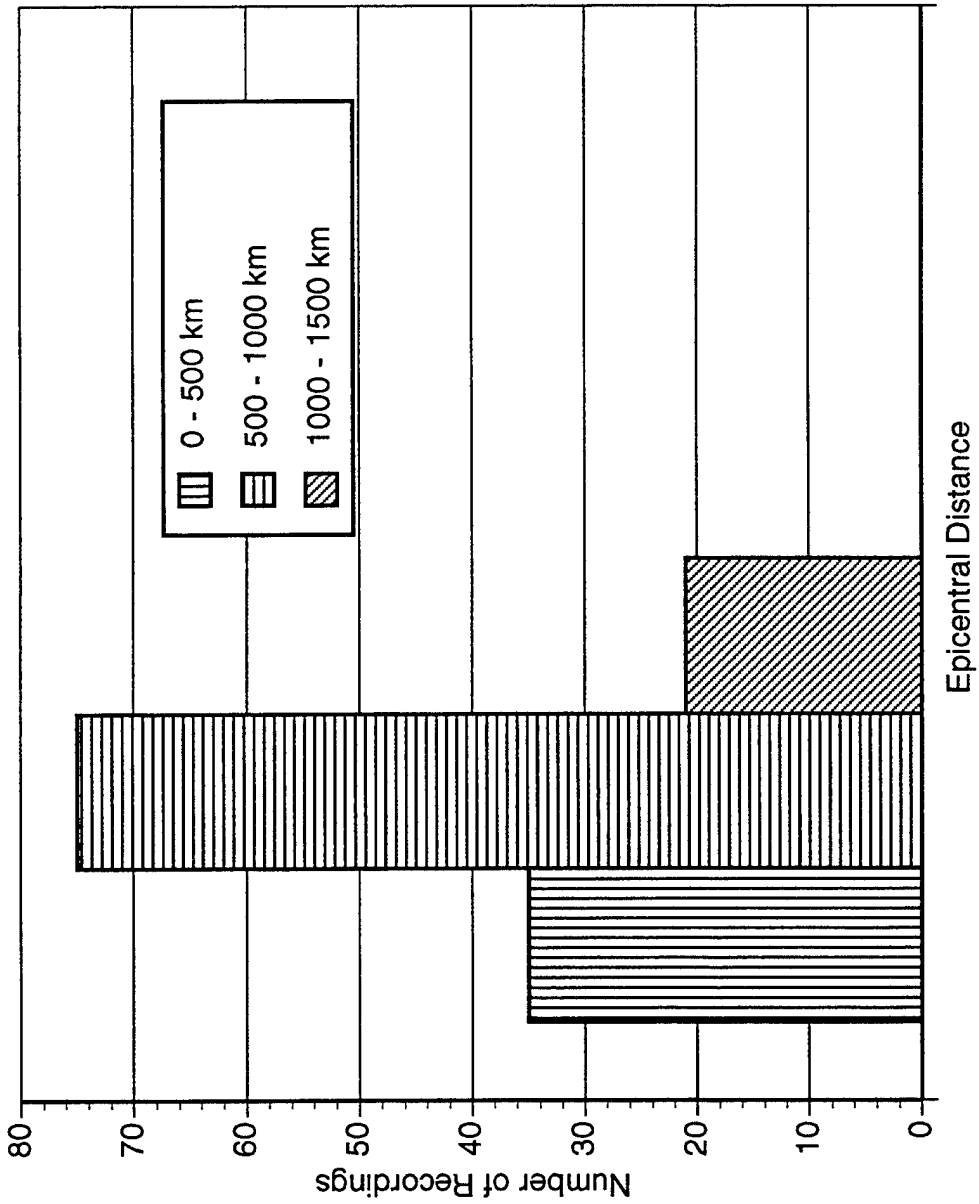


Figure 2. Distances of observations for selected NTS nuclear explosions and stations providing good digital waveforms at regional distances which are currently in the database.

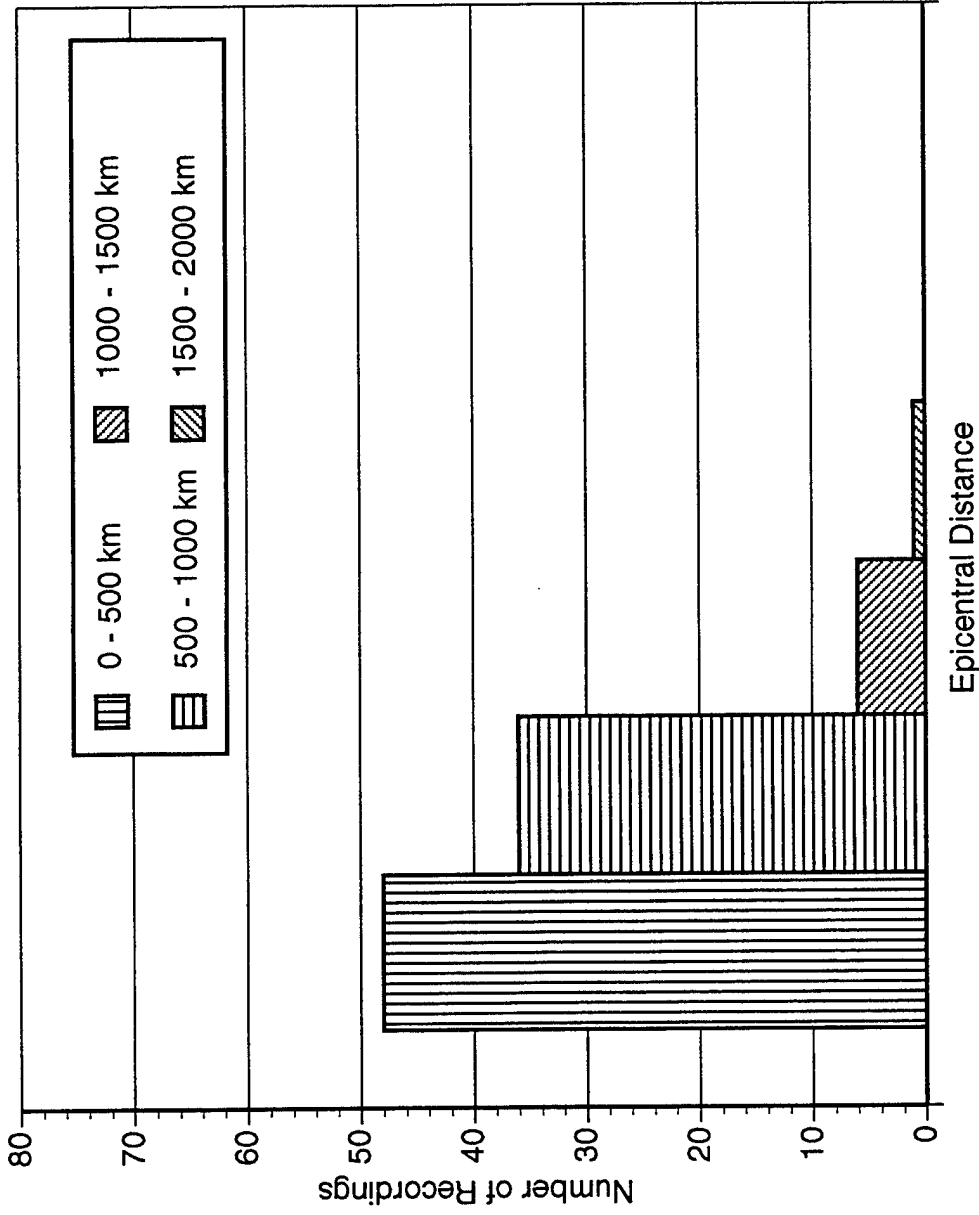


Figure 3. Distances of observations for selected western U.S. earthquakes and stations providing good digital waveforms at regional distances which are currently in the database.

LLNL stations are all at ranges less than 500 km, so we could easily expand the sample in this range with additional events from the LLNL network if needed. The VELA stations were at distances from 500 km to 1000 km from NTS explosions; additional digital data from these sources would be very difficult to acquire. However, this distance range also includes a large sample of NTS explosions recorded at the SRO station ANMO, and there also should be good quality regional recordings in this distance range from the station at Pinedale, Wyoming from many NTS nuclear explosion tests if additional events in this range are needed. Most of our NTS explosion data at ranges from 1000 km to 1500 km is from the RSTN station RSSD; additional NTS explosion data in this distance range could be acquired from the station at Lajitas, Texas. NTS explosions are recorded in North America at ranges beyond 1500 km, but relatively high attenuation in the western U.S. severely depletes regional seismic phases (particularly at high frequencies) and minimizes their value as potential discriminants at these far-regional distances. Therefore, we have made no attempt to use observations at stations beyond 1500 km from western U.S. events in our regional discrimination studies.

With regard to the earthquake distribution in Figure 3, all the LLNL station data in our current database is for ranges less than 500 km. We selected only events from the immediate vicinity of NTS; the database could be supplemented with more recent earthquakes near the test site and with additional other western U.S. earthquakes farther from NTS recorded at the same LLNL stations. The earthquake data at the VELA stations in our database fall into the ranges from 0 km to 500 km and from 500 km to 1000 km in Figure 3. It would be very difficult to supplement the database with additional earthquakes from the VELA stations; however, the Pinedale and Texas array stations and the RSSD station as well as other modern digital stations in the region could

provide useful supplements to the regional data in this distance range for western U.S. earthquakes.

### **2.3 Eurasian Event and Station Locations**

Figure 4 shows the locations of stations for which we have digital data in our current regional database for Eurasia relative to the principal nuclear test sites at Shagan River (SR) in East Kazakhstan, NZ on Novaya Zemlya, and Lop Nor in China. Figures 5 and 6 show the distributions with respect to epicentral distance for observations of nuclear explosions and earthquakes from the current regional database that we have assembled for regional discrimination studies in Eurasia. The data currently include digital recordings at selected Chinese Digital Seismic Network (CDSN) and Incorporated Research Institute for Seismology (IRIS) stations from events at the principal Asian test sites, PNE's throughout the former Soviet Union recorded at station Borovoye (BRV), and comparison data for earthquakes, which tend to be concentrated along the southern Soviet border.

In comparison to Figures 2 and 3, the observations from the Eurasian events generally cover broader ranges of epicentral distances. Whereas the western U.S. observations tend to be from ranges less than 1000 km, most of the Eurasian observations are for ranges greater than 1000 km. The reasons for this are that regional recordings at nearer stations have not been available for nuclear tests in the former Soviet Union and lower attenuation in Eurasian platform regions often allows the regional phase signals to be seen above the noise level at far-regional stations. Supplemental digital data may be available in certain distance ranges for some Eurasian nuclear explosions. The database does not currently include recordings at the Borovoye station of nuclear tests at the former Soviet test site in East Kazakhstan which could add to observations

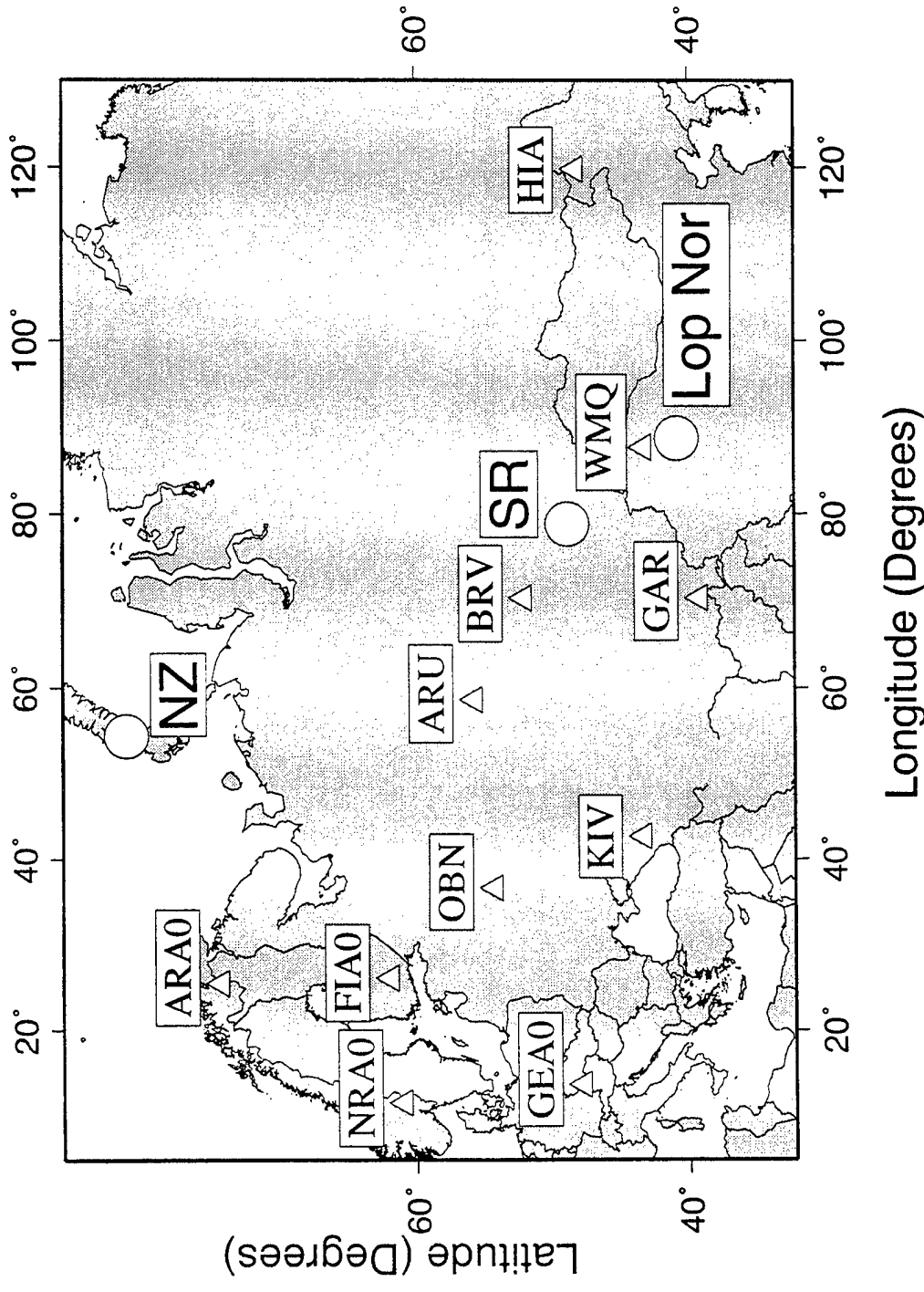


Figure 4. Map of Eurasia showing location of principal nuclear test sites relative to regional stations with good digital data which are currently in the database.

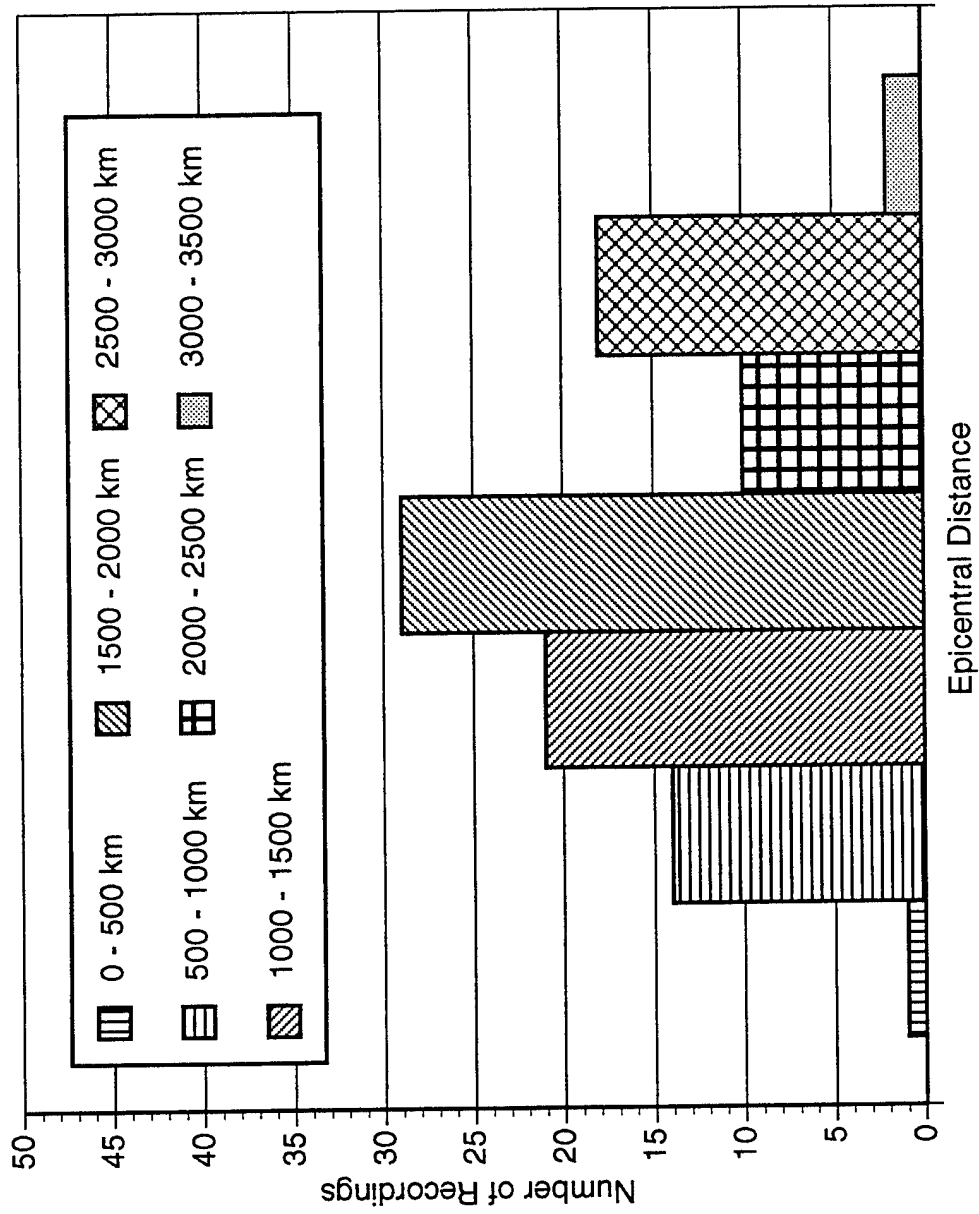


Figure 5. Distances of observations for selected Asian nuclear explosions and stations providing good digital waveforms at regional distances which are currently in the database.

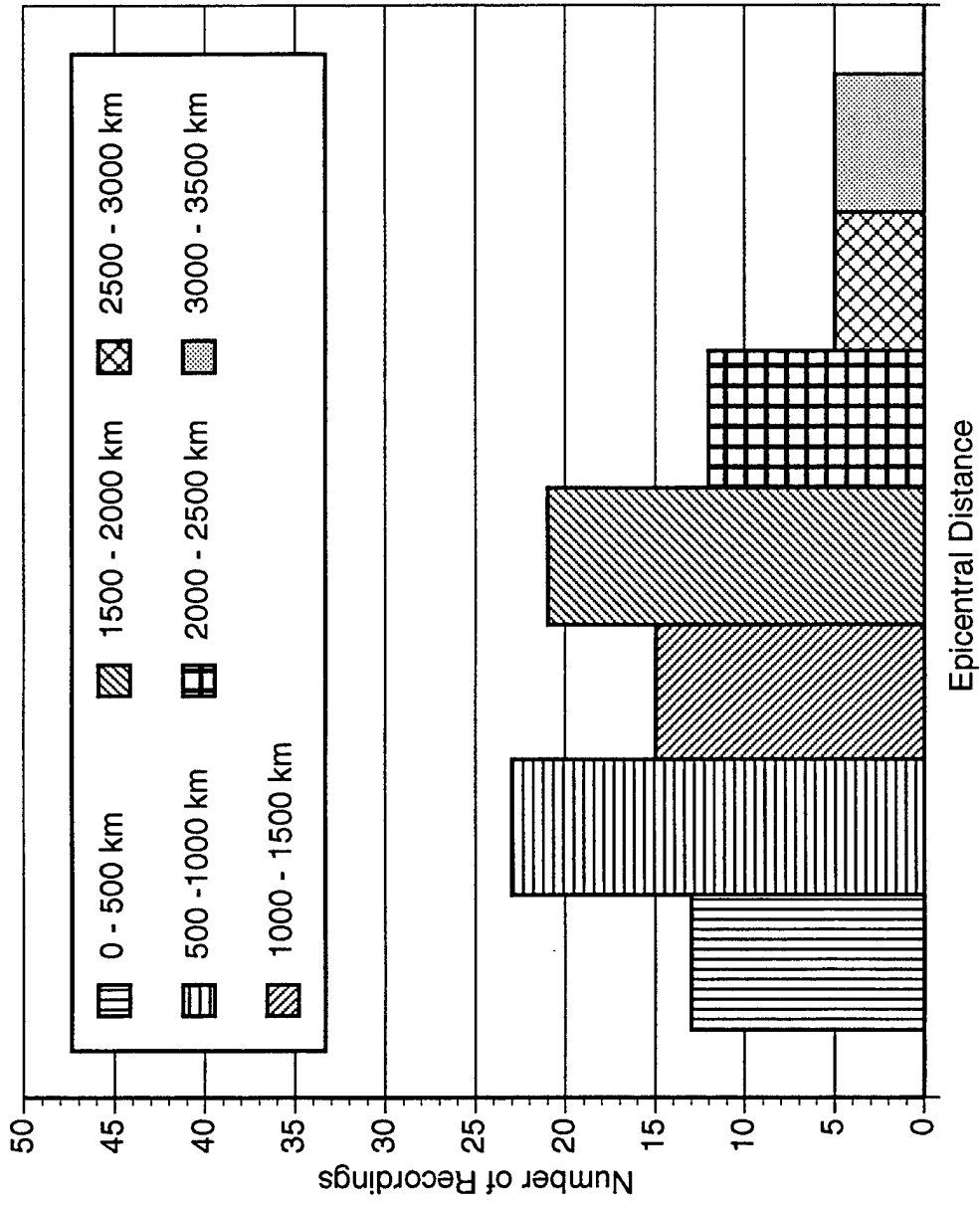


Figure 6. Distances of observations for selected Eurasian earthquakes and stations providing good digital waveforms at regional distances which are currently in the database.

in the 500 km to 1000 km range. There should also be regional data at additional Eurasian stations outside of China for some of the more recent Chinese nuclear tests at Lop Nor. Recent earthquake digital records from many modern regional stations could be used to supplement the data sample in almost any distance range desired; however, the earthquake locations are often different from those of the underground nuclear explosion tests. The most relevant earthquake data are probably those from areas of interest or with propagation paths similar to those from explosion sources. We are currently evaluating where supplemental data would be most useful.

#### **2.4 Regional Event Magnitudes**

Figures 7 and 8 show the distributions with respect to magnitudes for events in our western U.S. and Eurasian regional data samples. For the western U.S. the nuclear explosion sample includes magnitudes over the range from 3.5  $m_b$  to 6  $m_b$  with most events in the 5 - 5.5  $m_b$  range. The western U.S. earthquakes in our database tend to have lower magnitudes, with most events in the 3.5 - 4  $m_b$  range. The reason for this is that we tried to select earthquakes closer to NTS, and many of these were of lesser magnitude than the NTS nuclear tests to which they are being compared. In our analyses we have been attempting to minimize the significance of this discrepancy in two ways. First, we have been trying to add to the regional database earthquakes with somewhat higher magnitudes (viz. 4.5 - 5.5  $m_b$ ). Some more recent events on or just to the west of NTS have been recorded at several regional stations and should provide useful supplemental data. In addition, when comparing larger magnitude NTS explosions with the smaller earthquakes near NTS, we have analyzed the influence of source size on the observations using explosion source scaling techniques to make the explosions more comparable to the

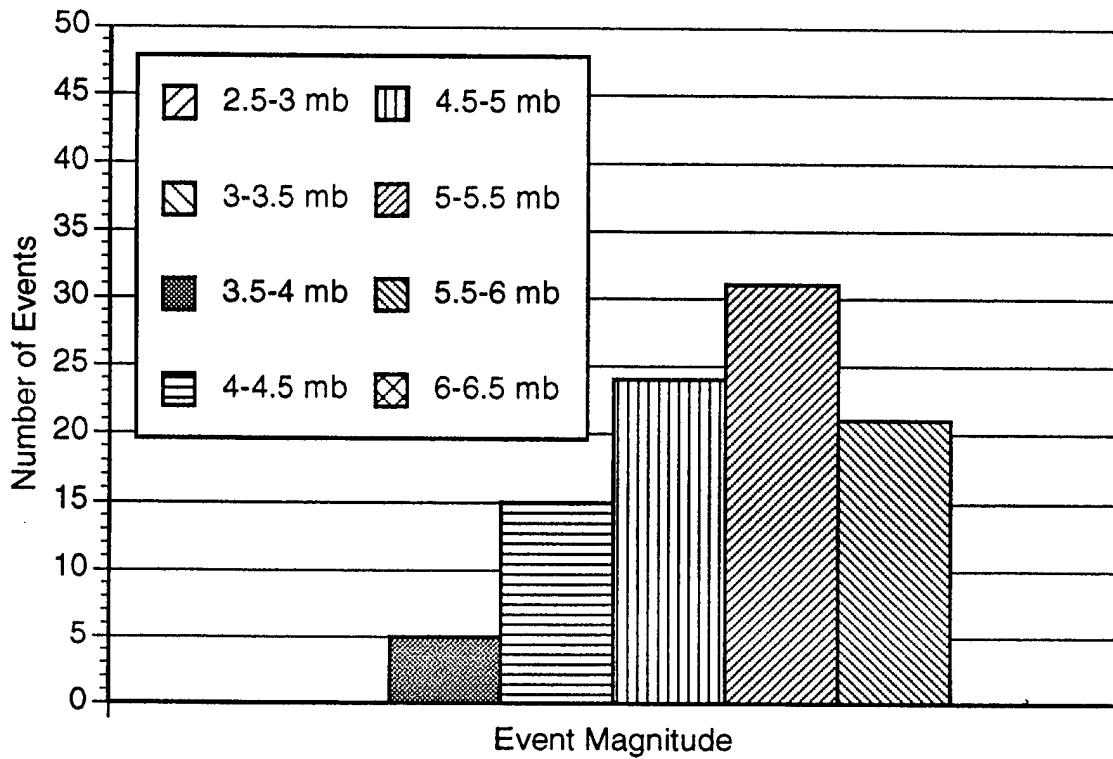


Figure 7(a). Distribution of western U.S. nuclear test observations in regional database with respect to event magnitude.

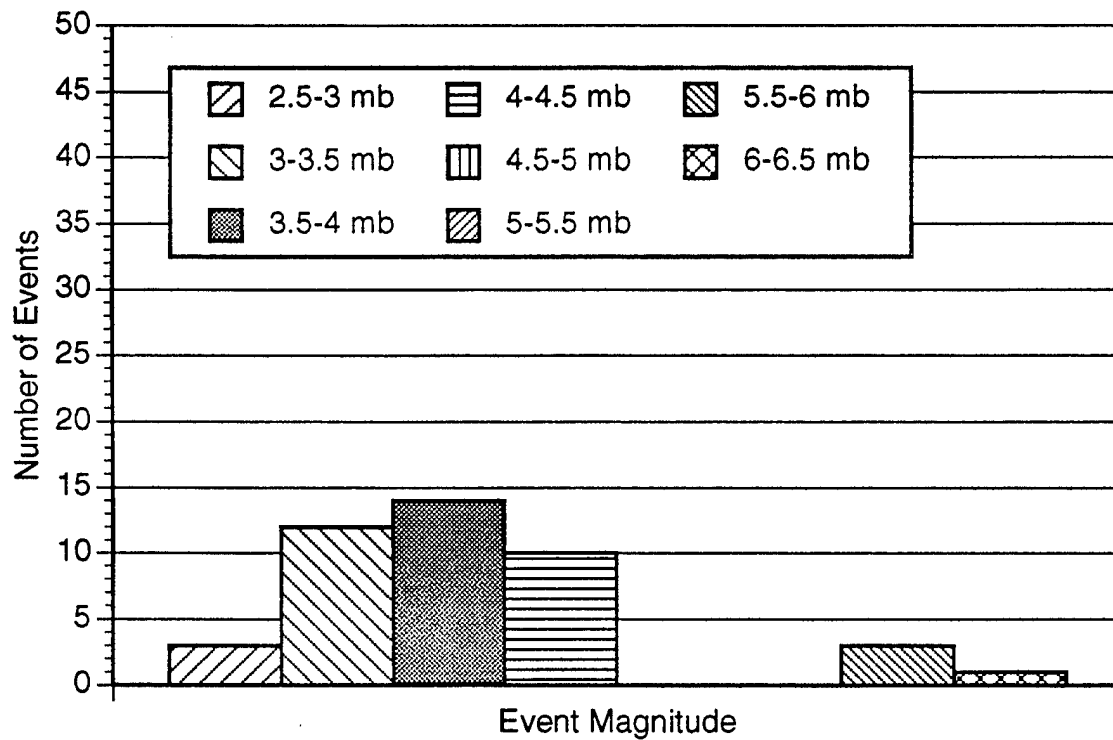


Figure 7(b). Distribution of western U.S. earthquake observations in regional database with respect to event magnitude.

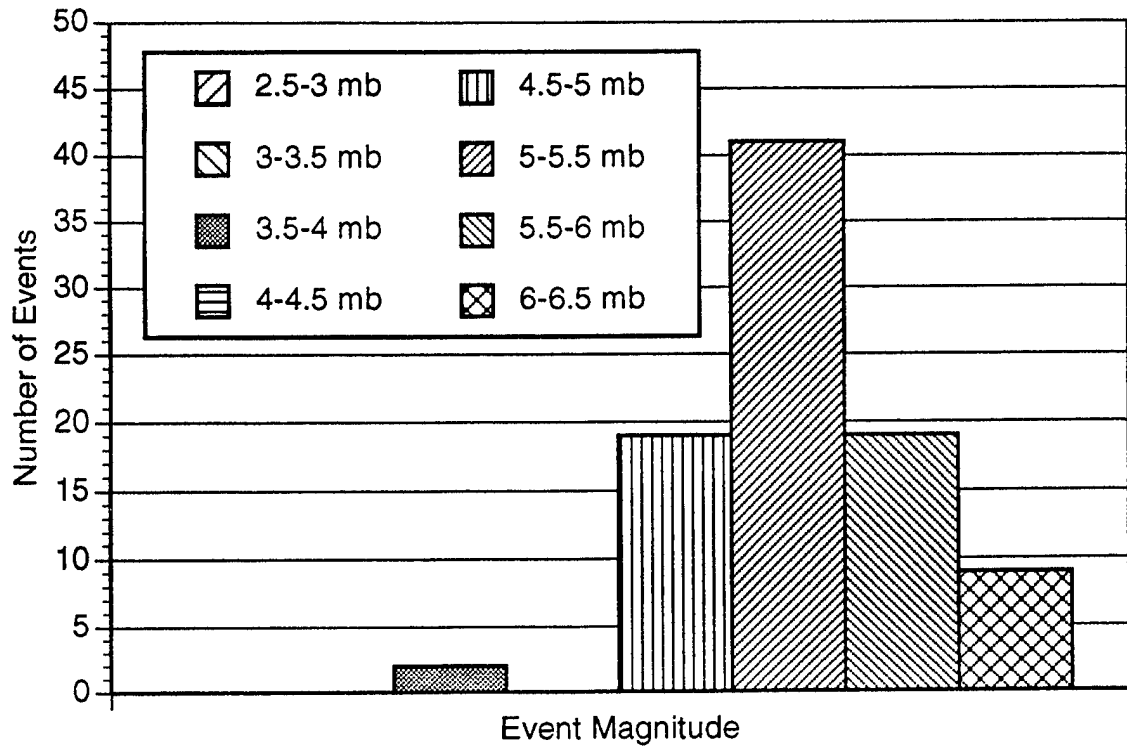


Figure 8(a). Distribution of Eurasian nuclear test observations in regional database with respect to event magnitude.

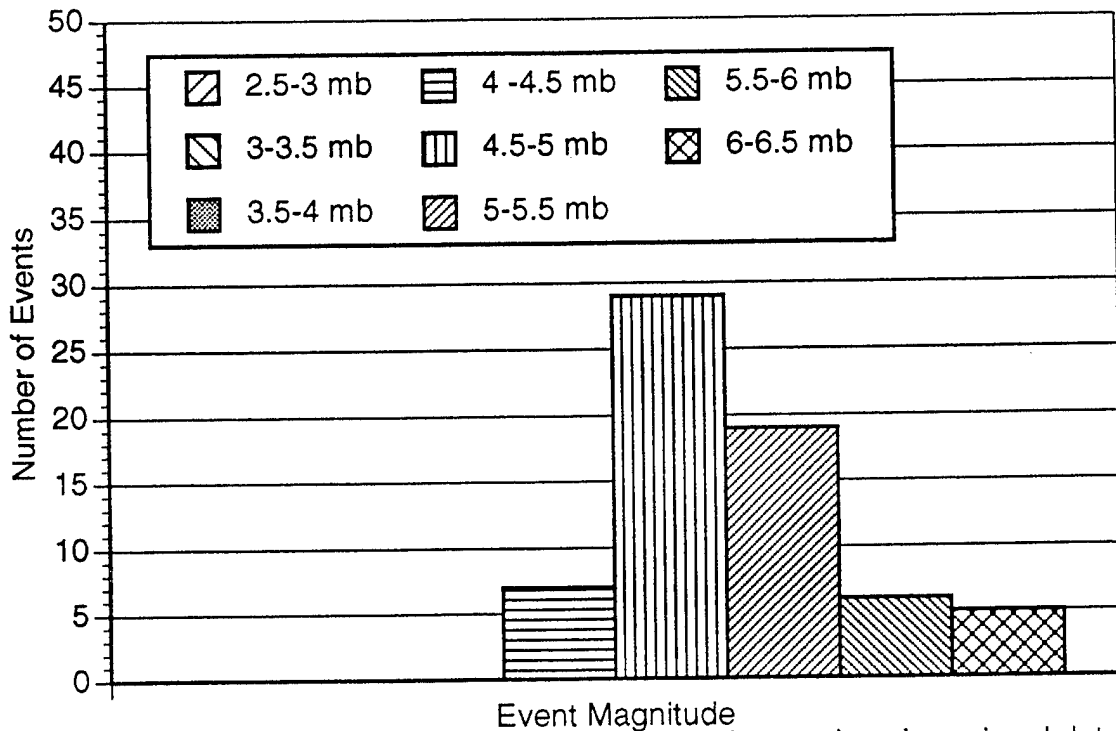


Figure 8(b). Distribution of Eurasian earthquake observations in regional database with respect to event magnitude.

earthquakes with respect to magnitude, as will be described in the following section.

The Eurasian nuclear test and earthquake magnitudes in Figure 8 show more overlap, although the nuclear tests again have somewhat higher magnitudes than the earthquakes in our samples. The Eurasian nuclear test magnitude distribution is peaked in the range 5 - 5.5  $m_b$ , while the earthquake magnitude distribution is peaked in the range 4.5 - 5  $m_b$ . Here too we are attempting to account for the influence of such magnitude differences on potential discriminant measures using source scaling techniques.

### **3. Further Analysis of Western U.S. Data**

#### **3.1 Previous Findings**

The original development of regional phase spectral ratios as discriminants (cf. Ryall, 1970; Murphy and Bennett, 1982) was based primarily on analysis of near-regional (ranges less than 800 km) signals from NTS nuclear explosions and earthquakes in the western U.S. Ryall (1970) found that the peak spectral amplitudes occurred at different frequencies for a small number of explosions and earthquakes recorded in Nevada at very near regional distances. Murphy and Bennett (1982) and Bennett and Murphy (1986) analyzed the near-regional VELA station data, described above in Section 2, from NTS explosions and nearby earthquakes and found that the earthquake regional phases, and especially L<sub>g</sub>, were relatively enriched in high frequencies compared to the explosions. These findings were confirmed by the studies of Taylor et al. (1988, 1989) for a large sample of NTS explosions and earthquakes throughout the western U.S. recorded at the LLNL stations surrounding NTS; and Bennett et al. (1989) found that subsets of the regional phases from the LLNL earthquake sample, for events nearer NTS, were also enriched in high frequencies compared to the explosions. While this discriminant seemed very promising, attempts to apply it in other regions have not always been so successful (cf. Bennett et al., 1989, 1992); and we have only a partial understanding of the theoretical reasons for the behavior observed in the NTS region.

#### **3.2 Analysis Procedures**

In the first phase of this research project, we decided to conduct some further analyses of the western U.S. events in the database. In particular, we have applied some alternative spectral analysis methods to the regional signals

at the LLNL network stations for selected NTS explosions and earthquakes. Figure 9 shows the locations of ten NTS nuclear explosions and eight earthquakes in the surrounding region which were recorded by the LLNL network. It should be noted that several of the nuclear tests are nearly coincident, and three of the earthquakes are at approximately the same location (viz. 37.26 N 115.08 W) and appear as only two squares on the map. In general, the earthquakes are close enough to the explosion sources, so that the regional propagation paths to the stations would be similar, and we would not expect significant differences in the spectra from regional phase propagation.

In our previous analyses of the western U.S. regional phase signals, we used standard Fourier analysis techniques to obtain spectral estimates. In the current research we have been seeking to define alternative processing procedures which might be useful for obtaining spectral estimates on a routine basis for a variety of regional phases. Such routine procedures could be useful in processing the large data streams currently being collected or planned for CTBT monitoring. The procedure which we have implemented is based on band-pass filter analysis of the regional waveforms. In most of these analyses, we have used a traditional band-pass filter process with fairly broad, overlapping filter passbands (cf. Bennett et al., 1989, 1996).

Figure 10 shows the results of the bandpass filter analysis applied to the vertical-component record at the LLNL station KNB for the NTS nuclear explosion GORBEA. At this distance range (viz. 290 km) the initial arrival is a relatively weak, emergent  $P_n$  phase which is followed about 5 seconds later by a strong but complex  $P_g$  signal. There is no clear  $S_n$  on the vertical-component record, but a strong  $L_g$  starts arriving about 35 seconds after the initial  $P_n$ . This  $L_g$  is the strongest signal on the record and has a long duration. Also, apparent on the record for the lowest frequency passband (viz. 0.01 - 0.1 Hz) is a long-

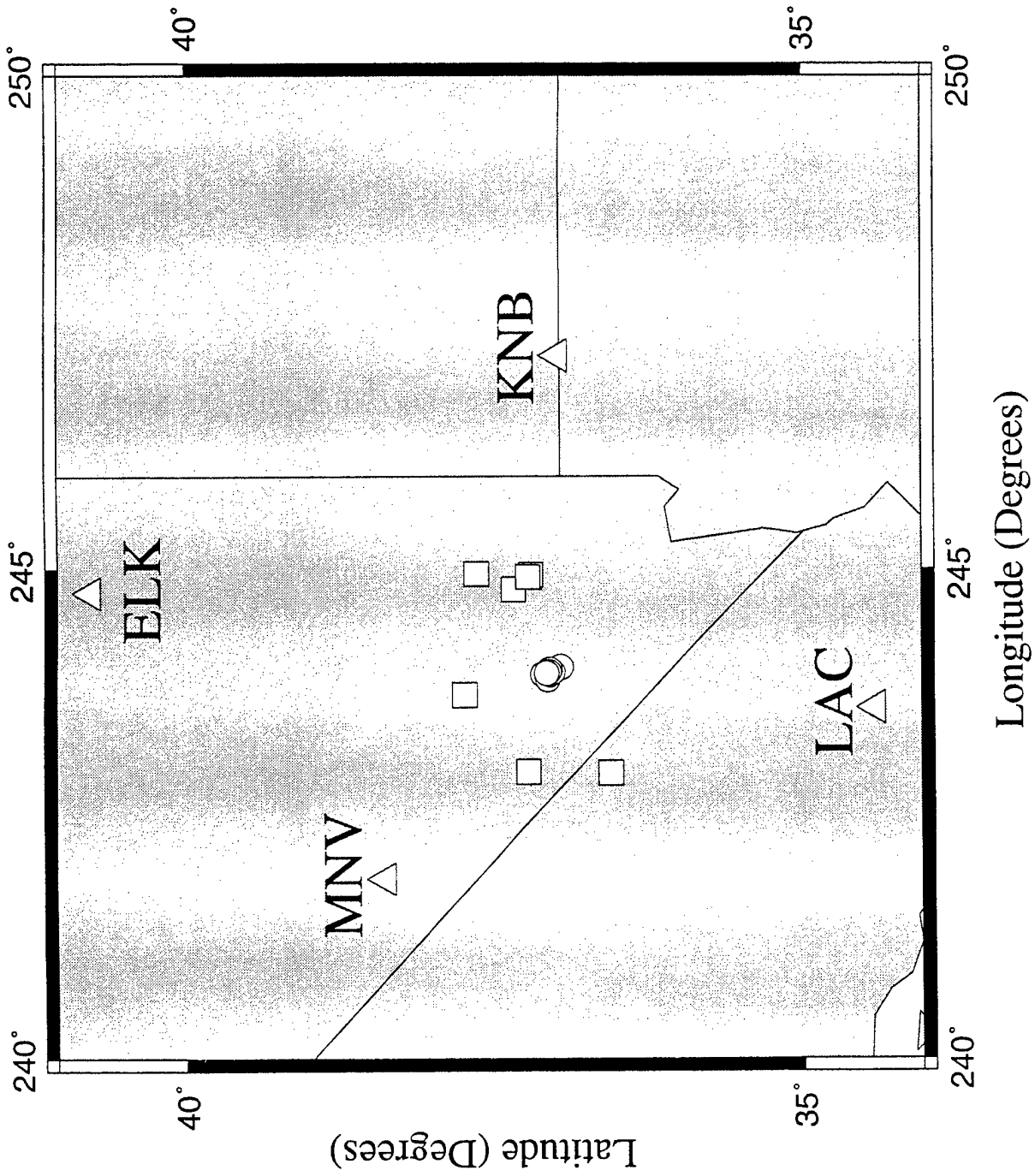


Figure 9. Map showing the locations of NTS nuclear explosions and nearby earthquakes relative to the LLNL network stations.

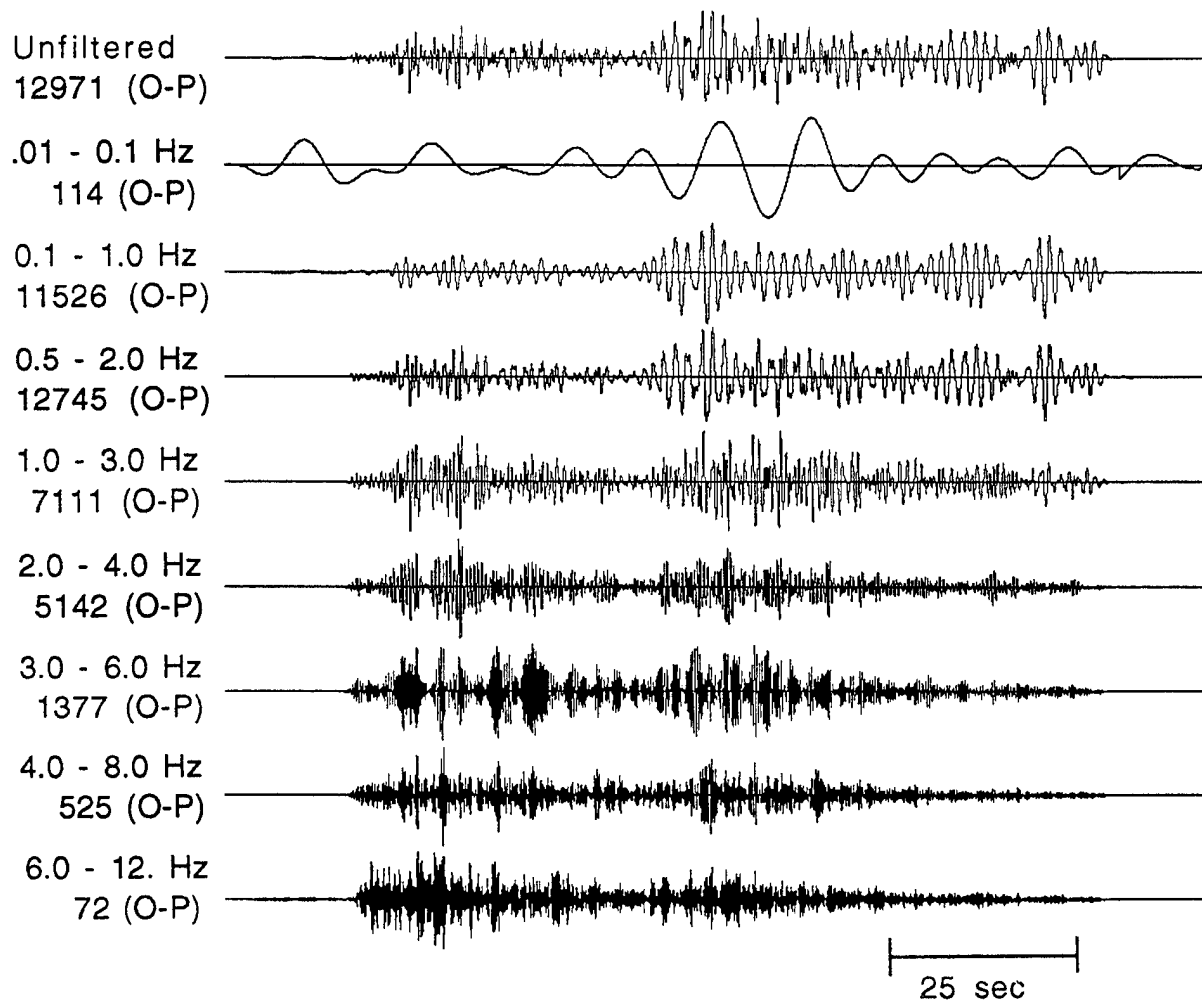


Figure 10. Traditional bandpass filter analysis of NTS explosion GORBEA recorded at station KNB.

period, fundamental-mode Rayleigh wave with indistinct onset arriving at about the same time as  $L_g$ .

For comparison we show in Figure 11 the results of the same bandpass filter analysis applied to the KNB record for the May 12, 1982 earthquake at a distance range of 205 km. At this somewhat smaller distance range, there is little separation between the  $P_n$  and  $P_g$  phases. There is again little evidence of  $S_n$ ; but a strong  $L_g$  signal, arriving about 25 seconds after the initial P, is the largest regional phase on the records. At frequencies near 1 Hz, there also appears to be a regional phase arriving after  $L_g$  and extending the signal duration. It seems unlikely that this is  $R_g$  unless the earthquake was unusually shallow. A more probable explanation is that non-direct propagation paths increase the  $L_g$  duration in this complex geologic environment. In the lowest frequency band there is again evidence of the long-period fundamental-mode Rayleigh wave from this earthquake.

We obtained relative spectral estimates from the band-pass filter results by comparing the amplitudes in the various frequency bands from the filtered output for a group velocity window corresponding to the regional phase of interest. For the broad filters used in Figures 10 and 11, our preliminary spectral estimation scheme is to simply measure the maximum peak motion amplitude from the filtered output in the appropriate group velocity window and then normalize by dividing by the maximum amplitude in the passband 0.1 - 1.0 Hz. We then plot the normalized spectral estimate at the center frequency of the filter passband. In fact, the relative spectra represent a form of spectral ratio - i.e. the ratio of the amplitude in a high-frequency passband to that in the low-frequency passband (viz. 0.1 - 1.0 Hz) used to normalize the spectral amplitudes. Thus, the relative spectra show the effect of computing the regional phase spectral ratio in different frequency bands.

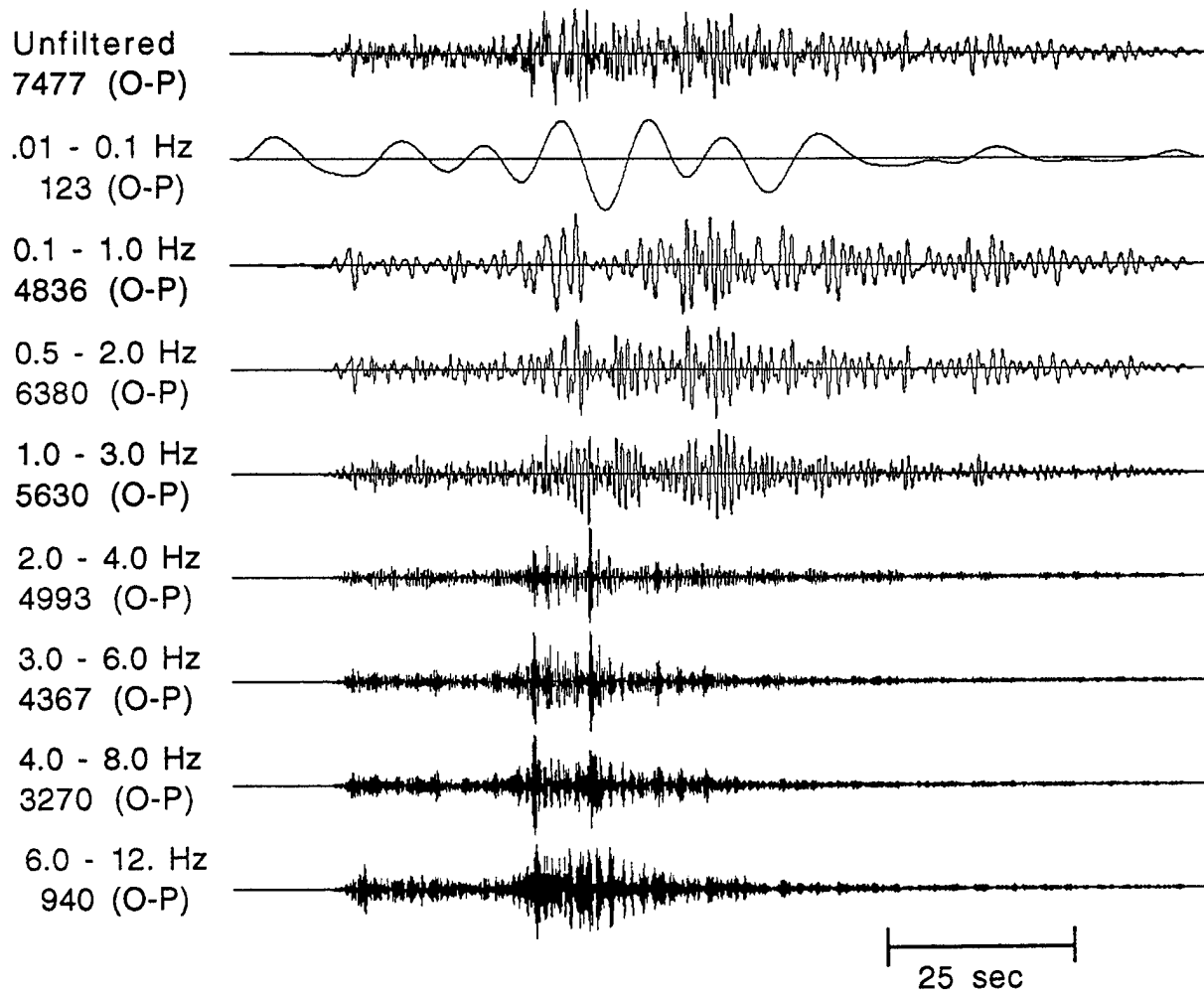


Figure 11. Traditional bandpass filter analysis of May 12, 1982 earthquake near NTS recorded at station KNB.

Figure 12 shows the relative spectral estimates corresponding to the  $L_g$  signals determined using this approach for the GORBEA NTS nuclear explosion and the 05/12/82 earthquake observed at station KNB. Focusing on the curves with the solid symbols, we note that the  $L_g$  spectral estimates tend to fall-off much more rapidly with increasing frequency for the nuclear explosion test than for the earthquake. The  $L_g$  spectral estimates for the earthquake are at or near 1.0 out to a center frequency of 4.5 Hz and slowly decline above that, while the explosion spectral estimates drop-off from 1.0 to about 0.1 at 4.5 Hz and continue to fall to below 0.01 at 9 Hz.

We have also been considering several alternative schemes for spectral estimation. One such scheme uses a set of narrower Gaussian filters spaced at closer frequency intervals. In this alternative procedure, instead of simply measuring maximum amplitude in the group velocity window, we compute a RMS average of the amplitudes within the selected group velocity range. The amplitudes are again normalized by dividing by the average amplitude at about 0.55 Hz to obtain the relative  $L_g$  spectral estimates which are plotted with the hollow symbols in Figure 12. The alternative spectral estimates generally fall below and drop-off more rapidly with frequency than the original spectral estimates; these alternative spectra also generally appear less smooth. This probably results because the original, broader filters tend to average over the wider frequency band and average in more low-frequency energy in the  $L_g$  signals. At frequencies of about 2.5 Hz and above, we see about the same separation between the explosion and earthquake using the alternative estimates as we found using the original spectral estimation methods. However, at lower frequencies (below about 2 Hz) the explosion and earthquake  $L_g$  spectra show little separation. This suggests that the differences in the spectra that are seen at lower frequencies for the original spectral

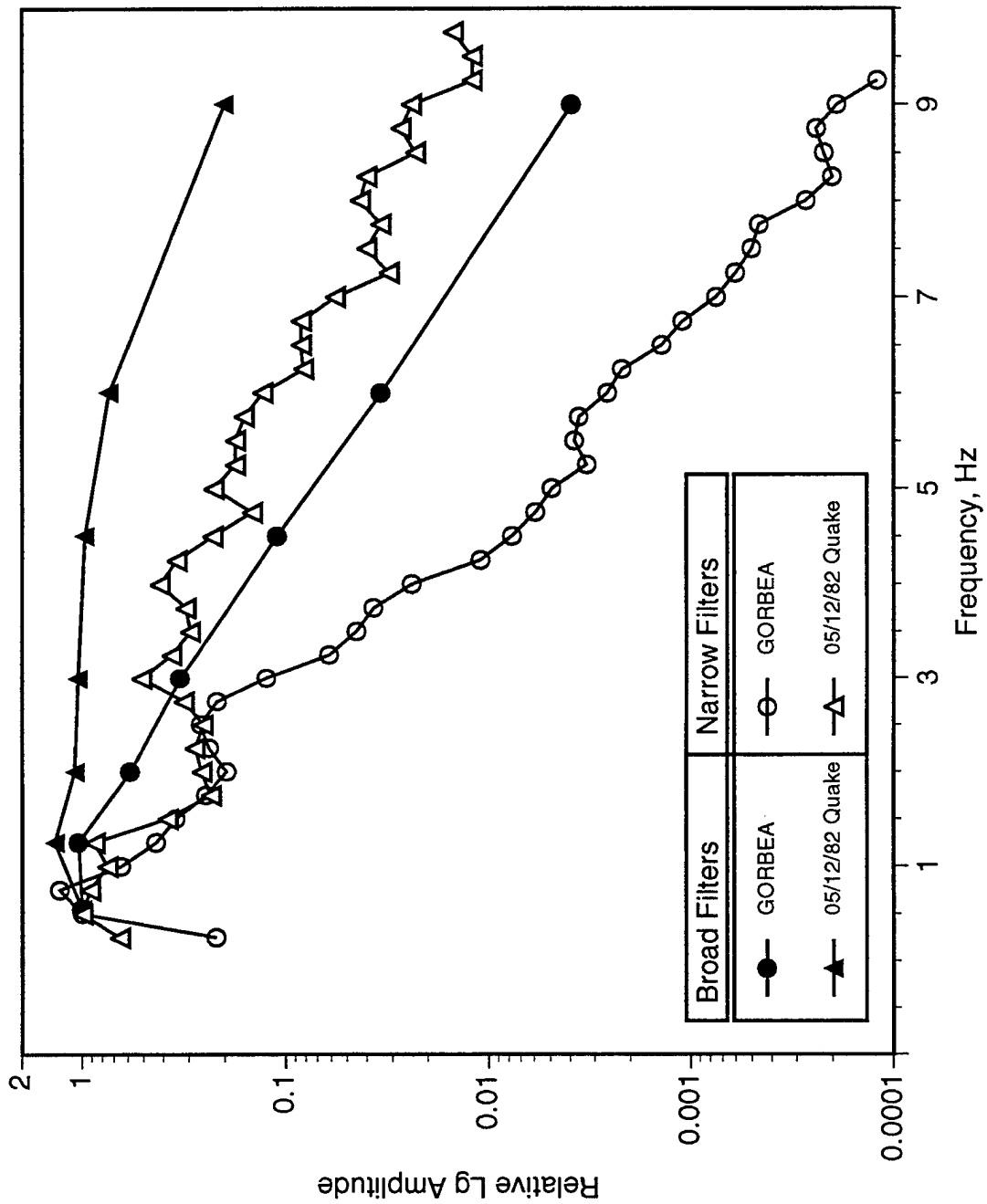


Figure 12. Comparison of Lg spectral estimates at station KNB for broad traditional bandpass filters and narrow Gaussian filters for nuclear test GORBEA and 05/12/82 earthquake.

estimation scheme could be caused by the broad filters including some of the higher-frequency differences. We are continuing to consider a variety of alternative techniques for determining regional phase spectral estimates; but, in the remainder of this report, we use the broader traditional filters to provide a consistent comparison between the relative spectral measurement for the events in different areas.

### **3.3 Application to Western U.S. Event Samples**

In our initial analysis phase, we have focused on five NTS nuclear explosion tests and five nearby earthquakes recorded by the four LLNL stations. The epicentral distances for these nuclear tests were between 230 km and 410 km, while the distances for the earthquakes were between 180 km and 490 km. Magnitudes for the explosions were between 4.1  $m_b$  and 5.7  $m_b$  (4.2  $M_L$  to 5.5  $M_L$ ); and magnitudes for the earthquakes were between 3.5  $M_L$  and 4.2  $M_L$  (most earthquakes had no reported  $m_b$ 's). Figure 13 shows the relative  $L_g$  spectral amplitudes, normalized to the value at 0.55 Hz (center frequency), for the five NTS nuclear tests and five nearby earthquakes recorded at station KNB. The relative  $L_g$  spectra are generally consistent with the behavior we saw above in Figure 12 comparing nuclear explosion GORBEA and the 05/12/82 earthquake. We see some variability in the spectra between events within a given source type, with the explosion scatter surprisingly appearing somewhat greater than that for the earthquakes. Variations in the explosion  $L_g$  spectral estimates are greatest at frequencies of 3 Hz and 4.5 Hz where they are about a factor of seven, while the greatest variations between earthquakes is about a factor of five at high frequencies.

Figure 14 shows a similar plot for the relative  $L_g$  spectra for five NTS nuclear tests and five earthquakes recorded at station MNV. In this case there

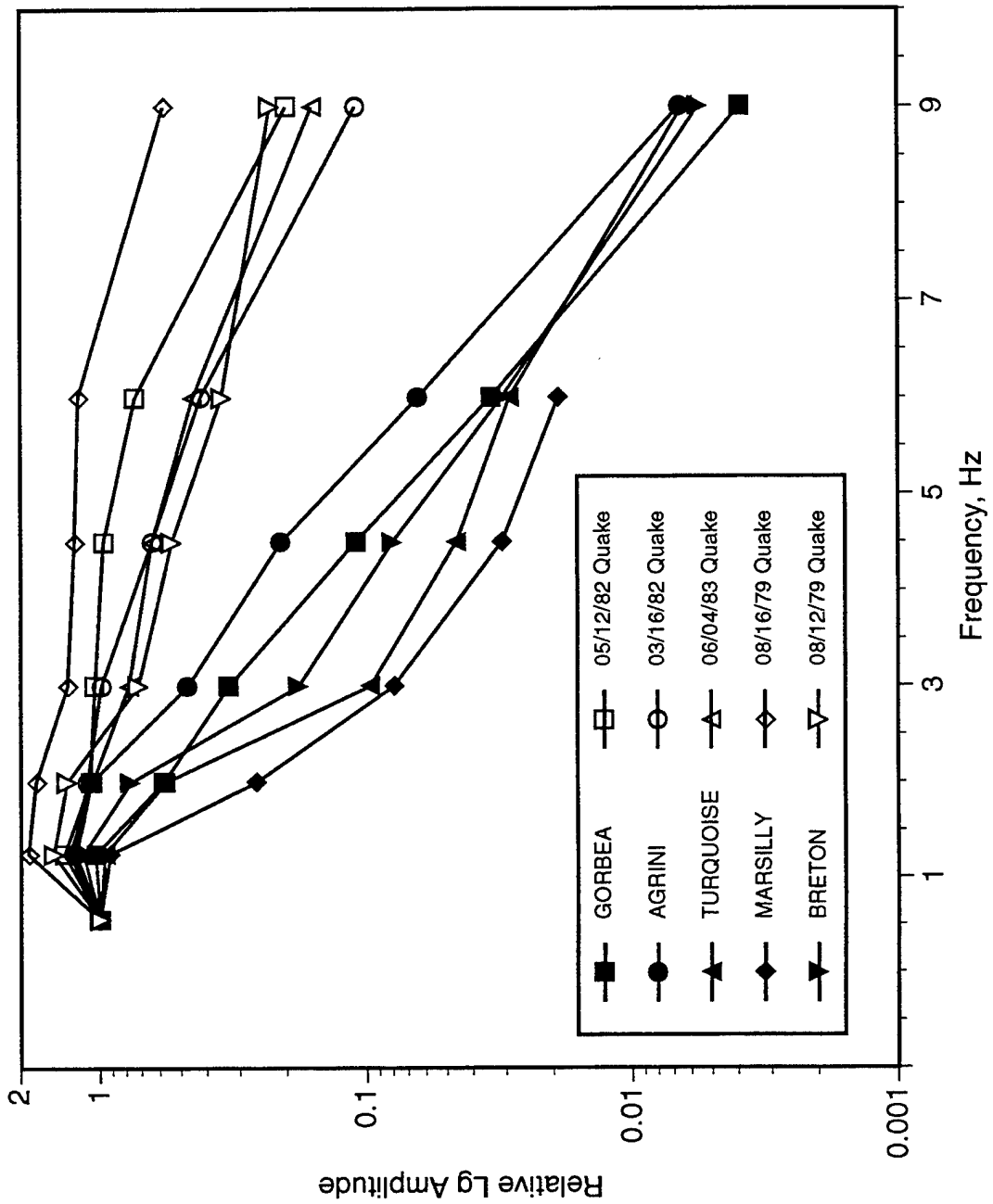


Figure 13. Relative Lg spectral estimates obtained for NTS nuclear tests and nearby earthquakes from traditional bandpass filter analyses of records at station KNB.

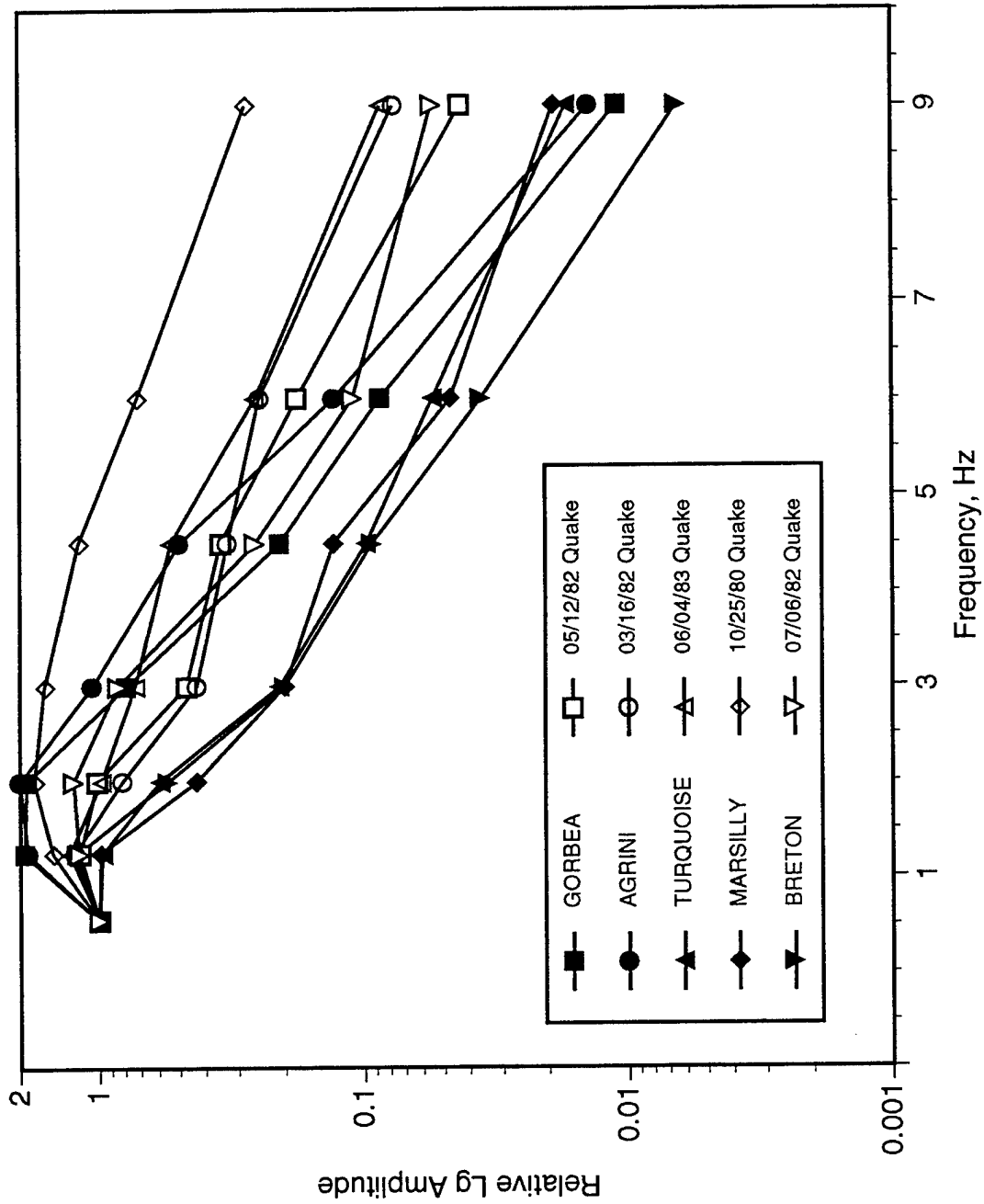


Figure 14. Relative Lg spectral estimates obtained for NTS nuclear tests and nearby earthquakes from traditional bandpass filter analyses of records at station MNV.

appears to be somewhat greater variability in the spectra for the earthquakes and less separation between the source types. Whereas we saw complete separation of source types in Figure 13 for KNB at frequencies of 3 Hz and greater, for MNV in Figure 14 we only see complete separation at the highest frequency (viz. the 6 - 12 Hz passband). This seems to be caused by higher spectral levels (i.e. spectral ratios) for the explosions and lower spectral levels for the earthquakes at MNV. This could be caused by propagation differences for the explosions and earthquakes, but there could also be a radiation pattern effect for the earthquakes.

### **3.4 Effects of Source Size on Regional Phase Spectra**

It is well known that source size can affect the spectra of regional phases (cf. Mueller and Murphy, 1971; Taylor, 1991; Chael, 1991; Walter and Priestley, 1991). In our original studies of regional phase spectral ratio discriminants (cf. Murphy and Bennett, 1982; Bennett and Murphy, 1986), we made an effort to select small explosions for comparison to the small earthquakes occurring near NTS. We also found that, when we plotted  $L_g$  spectral ratios as a function of magnitude, there was separation between the explosion and earthquake ratios over the magnitude range where the sample overlapped; and there was no evidence of any trend which would suggest that the measurements might converge at higher or lower magnitudes outside that range. Seismic source scaling (cf. Mueller and Murphy, 1971; von Seggern and Blandford, 1972; Walter and Priestley, 1991; Bennett et al., 1995) provides a way to directly test the expected influence of source size on regional phase spectral ratios. From Mueller-Murphy source-scaling theory (cf. Mueller and Murphy, 1971), we can predict that, when nuclear explosion tests are scaled from higher to lower yields, the high-frequency content of the seismic signals is enhanced relative to

the low-frequency content. We can then use the source-scaling theory to compensate for differences in source size.

As noted above, the NTS explosions at the LLNL stations used in Figure 13 are somewhat larger in magnitude than the earthquakes used for comparison. The average  $M_L$  difference is about 1.24 magnitude units, and we assumed a similar difference in  $m_b$  to perform the scaling. We applied the scaling procedures to the records for the five NTS explosions recorded at station KNB. Ideally in scaling we would use the individual event magnitude levels and scale to a common magnitude. In this case we used instead an approximate method with a single scaling function corresponding to the difference between the average magnitude of the explosions (viz. 4.92  $M_L$ ) and the average magnitude of the earthquakes (viz. 3.68  $M_L$ ). After scaling down the explosion records, we recomputed the relative regional phase spectra.

Figure 15 shows a comparison of the average  $L_g$  spectral estimates for the events recorded at station KNB before and after the scaling. The earthquake records are not scaled in this process, and their average values remain the same. The average earthquake  $L_g$  spectral amplitudes in Figure 15 are at 1.0 or slightly above at low frequencies and then slowly decline to a value near 0.3 at 9 Hz. On the other hand, the average  $L_g$  spectral amplitudes for the unscaled NTS nuclear tests had values near 1.0 at low frequencies but rapidly declined to a value less than 0.006 at 9 Hz. As expected, scaling the nuclear test records to lower magnitudes increases the relative high-frequency content in the regional signals. From 0.5 Hz to 2 Hz we see only very slight differences in the  $L_g$  spectral estimates between the scaled and unscaled records for the nuclear explosions. However, above 2 Hz the decline in the  $L_g$  spectra is much slower for the scaled records to a value near 0.04 at 9 Hz. So, the large differences between the NTS explosions and earthquakes at station KNB at

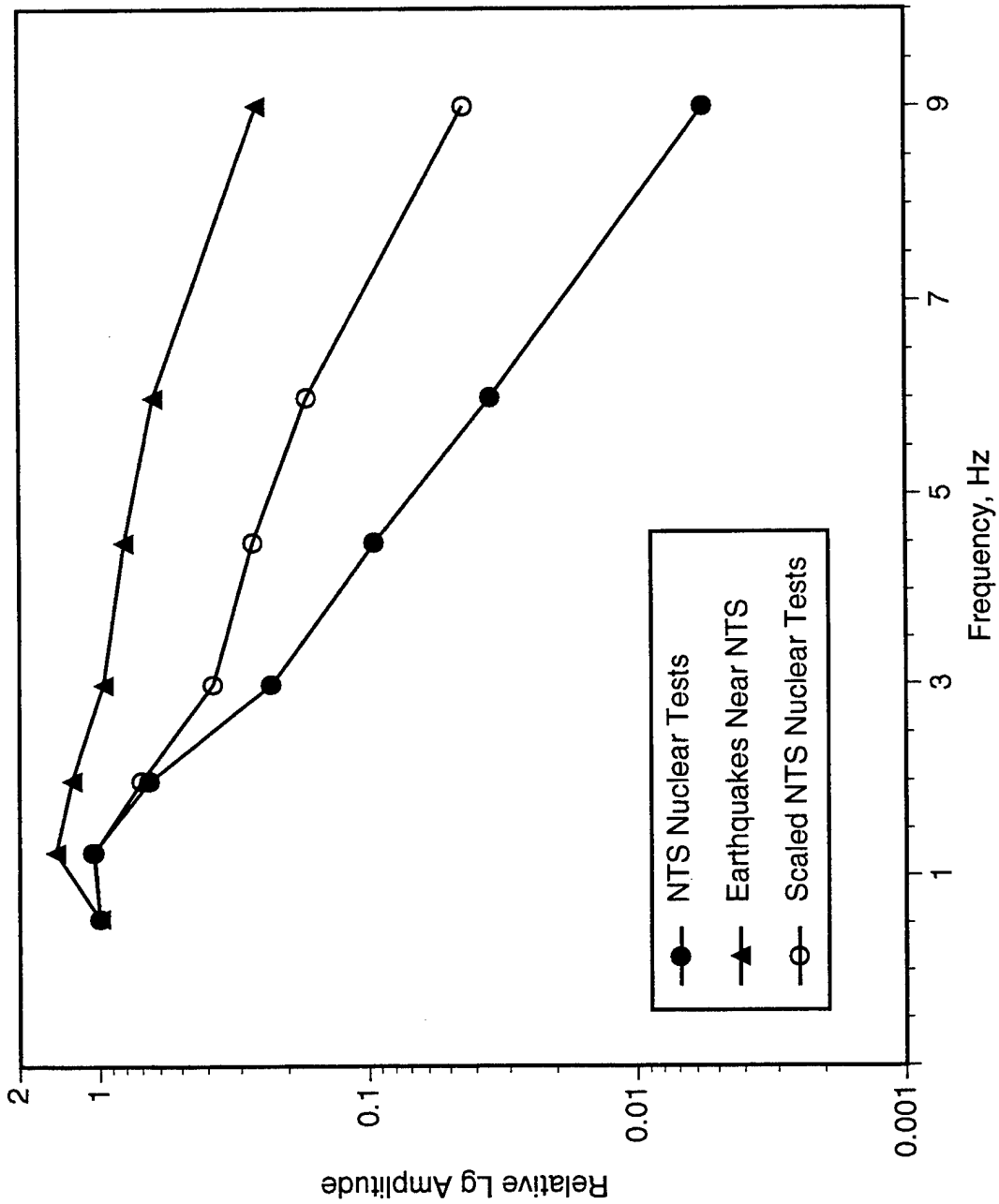


Figure 15. Comparison of average Lg spectral estimates at station KNB for 5 NTS nuclear tests, 5 nearby earthquakes, and 5 scaled NTS nuclear tests.

high frequencies is reduced by about a factor of eight when the average size difference between the events is accounted for by source scaling. However, it should be noted that the remaining difference in the average  $L_g$  spectra between the scaled nuclear tests and the earthquakes is still about a factor of six.

We haven't carried out the comparison completely for the  $L_g$  observations at station MNV; but we would expect the high-frequency content of the  $L_g$  signals for the scaled NTS explosions to be boosted by only a slightly smaller amount than at KNB, because the earthquake/explosion magnitude difference is not quite as great. However, since the difference in the average  $L_g$  spectral amplitudes between the earthquakes and unscaled explosions was only about a factor of eight to start with, it seems likely that much of the  $L_g$  spectral difference at station MNV between the earthquakes and scaled nuclear explosions would disappear. The differences in the spectral ratio estimates between stations suggests that discriminant measures of this type should probably not rely on single station observations, and that procedures to combine measurements from a network of regional stations should be investigated further.

In Figure 16 we show the same kind of scaling exercise except for the  $P_g$  signals at station KNB. The average  $P_g$  spectral amplitudes for the earthquakes have values of one and above out to 3 Hz, and there is a slow decline to a value near 0.4 at 9 Hz. The original average  $P_g$  spectral amplitudes for the unscaled NTS nuclear tests start out at low frequencies at one or above and decline more rapidly above 1 Hz to a value near 0.03 at 9 Hz. So, there is more than a factor of ten separation between the  $P_g$  spectra for the earthquakes near NTS and the unscaled NTS nuclear tests. However, after applying the Mueller-Murphy source scaling to make the NTS explosions more nearly equivalent in

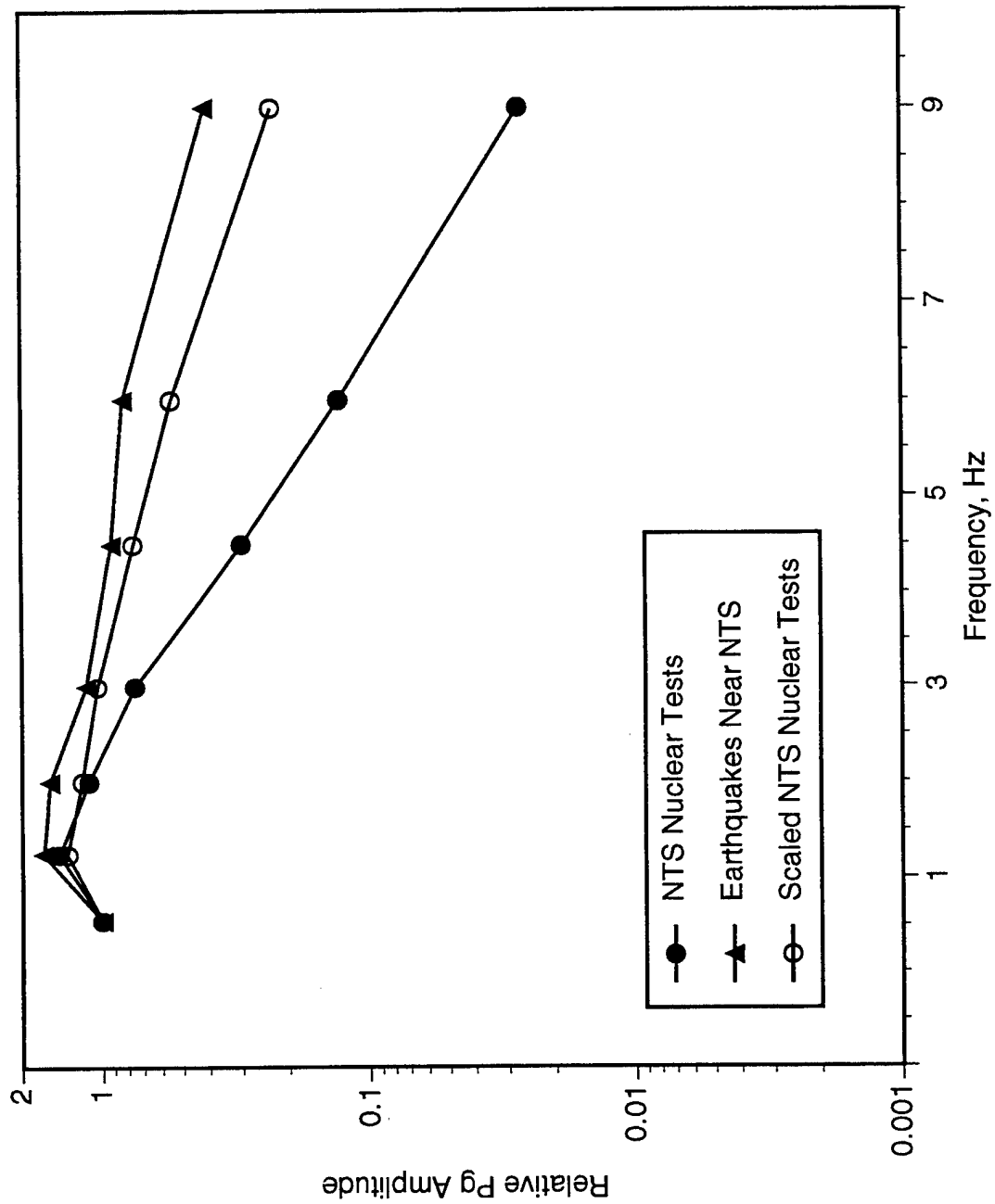


Figure 16. Comparison of average Pg spectral estimates at station KNB for 5 NTS nuclear tests, 5 nearby earthquakes, and 5 scaled NTS nuclear tests.

magnitude to the earthquakes, the differences in the  $P_g$  spectra are severely reduced. The maximum difference is only about a factor of two at 9 Hz and is very small at some frequencies.

## 4. Analyses of Asian Data

### 4.1 Previous Findings

An early objective in regional discrimination research was to extend the discriminant measures which worked in the western U.S. to other geographical regions. Much of this effort focused on the former Soviet Union (cf. Bennett et al., 1989, 1992), because of interest in the Soviet weapons testing program, and on Scandinavia and northern Europe (cf. Baumgardt and Young, 1990; Dysart and Pulli, 1990), because the prototype regional seismic arrays were located there. As noted above in Section 2, most regional recordings from Soviet nuclear tests have come from stations at far-regional distances. Furthermore, the earthquake signals which are available for comparison come from events which are usually not in the same area as the nuclear test sites.

Bennett et al. (1989, 1992) found evidence from Eurasian events suggesting that  $L_g/P$ , or  $S_{max}/P_{max}$ , amplitude ratios tended to fall-off more rapidly with increasing frequency for Shagan River nuclear tests than for earthquakes at comparable distances. Although this initially appeared to be consistent with observations in the western U.S. (i.e. similar  $P_n$  spectral shapes for explosions and earthquakes but earthquake  $L_g$  spectra richer in high frequencies), it was found that the  $L_g$  signals at WMQ had higher corner frequencies for explosions than for earthquakes of similar magnitude. Dysart and Pulli (1990) found that  $L_g/P$  ratios for chemical explosions and earthquakes in Scandinavia measured at regional array stations were similar at low frequencies but tended to be lower for the explosions at high frequencies. Baumgardt and Young (1990) found that  $L_g$  spectral ratios were not particularly effective for separating Scandinavian chemical explosions and earthquakes but that  $S/P$  ratios did seem to provide separation for some events, implying possible differences in the regional P-wave spectra. It is unclear to what extent

the observations from chemical explosions, such as those in Scandinavia, can be used to infer the behavior of regional phases for other types of explosions (viz. underground nuclear tests).

An additional factor complicating the findings cited above for Eurasia is what influence propagation differences may have on observed behavior for the various event types. Bennett et al. (1989) attempted to make some simple attenuation adjustments to the  $L_g$  spectral shapes based on  $Q$  models for Shagan River and Central Asia to compensate for path differences between the explosions and earthquakes recorded at station WMQ. Characteristics of regional phase propagation in Eurasia have been investigated by several authors (e.g. Nersesov and Rautian, 1964; Piwinskii and Springer, 1978; Nuttli, 1981; Kadinsky-Cade et al., 1981; Jih and Lynnes, 1992) and attenuation models have been identified for various phases, particularly for  $L_g$ , throughout much of Asia (cf. Xie and Mitchell, 1990). In the course of this research project, we have reviewed much of the published literature on regional phase signal propagation in Eurasia. It remains to define models for all regional phases of potential interest and to routinely apply propagation adjustments based on the attenuation models to determine the implications of such adjustments to various regional discriminant measures, and in particular to spectral ratio discriminants. As this research progresses we will draw upon results from the prior studies to adjust the procedures and measurements for propagation and thereby assess regional discriminant transportability.

#### **4.2 Application of Analysis Techniques to WMQ Records**

One of the nearest seismic stations to the former Soviet test site in East Kazakhstan for which we have good regional signals from a fairly large sample of events is the CDSN station WMQ. As part of the current research effort, we

have systematically applied the same spectral analysis techniques to several events from the WMQ data sample. Figure 17 shows the locations of five Shagan River nuclear tests and five earthquakes at about the same epicentral distance for which we obtained good regional signals at WMQ. As noted earlier, the earthquake records used for comparison come from events in somewhat different source areas and azimuths because the area surrounding the Shagan River test site has a low level of natural seismicity and has produced no earthquakes of comparable size to the nuclear tests there. We followed exactly the same procedures as described above in Section 3 to determine regional phase spectral amplitude estimates. The same set of bandpass filters was applied to the vertical component records, and the amplitudes were measured in the appropriate regional phase group velocity windows. The relative spectral amplitudes were then determined by taking the ratio of the measured amplitude to the amplitude measured in the same group velocity window for the passband from 0.1 Hz to 1 Hz.

Figure 18 shows the relative  $L_g$  spectral amplitude measured at WMQ for five Shagan River explosions. The spectra for all the explosions are tightly clustered and show nearly the same dependence on frequency. The spectra have maximum values near one at frequencies of 0.55 Hz and 1.25 Hz, and then show a rapid decline above 1.25 Hz. The spectra reach low values less than 0.005 at a frequency of 9 Hz. In analyzing these signals, we experimented a little with alternative group velocity bounds on the group velocity window in which the maximum amplitudes were picked for the  $L_g$  phase. In Figure 18 we used a traditional  $L_g$  group-velocity window extending from 3.6 km/sec to 3.0 km/sec for our spectral amplitude measurements. We also considered a group velocity window from 4.6 km/sec to 3.0 km/sec for the spectral measurements; this window would include more regional S phases including  $S_n$  prior to  $L_g$ .

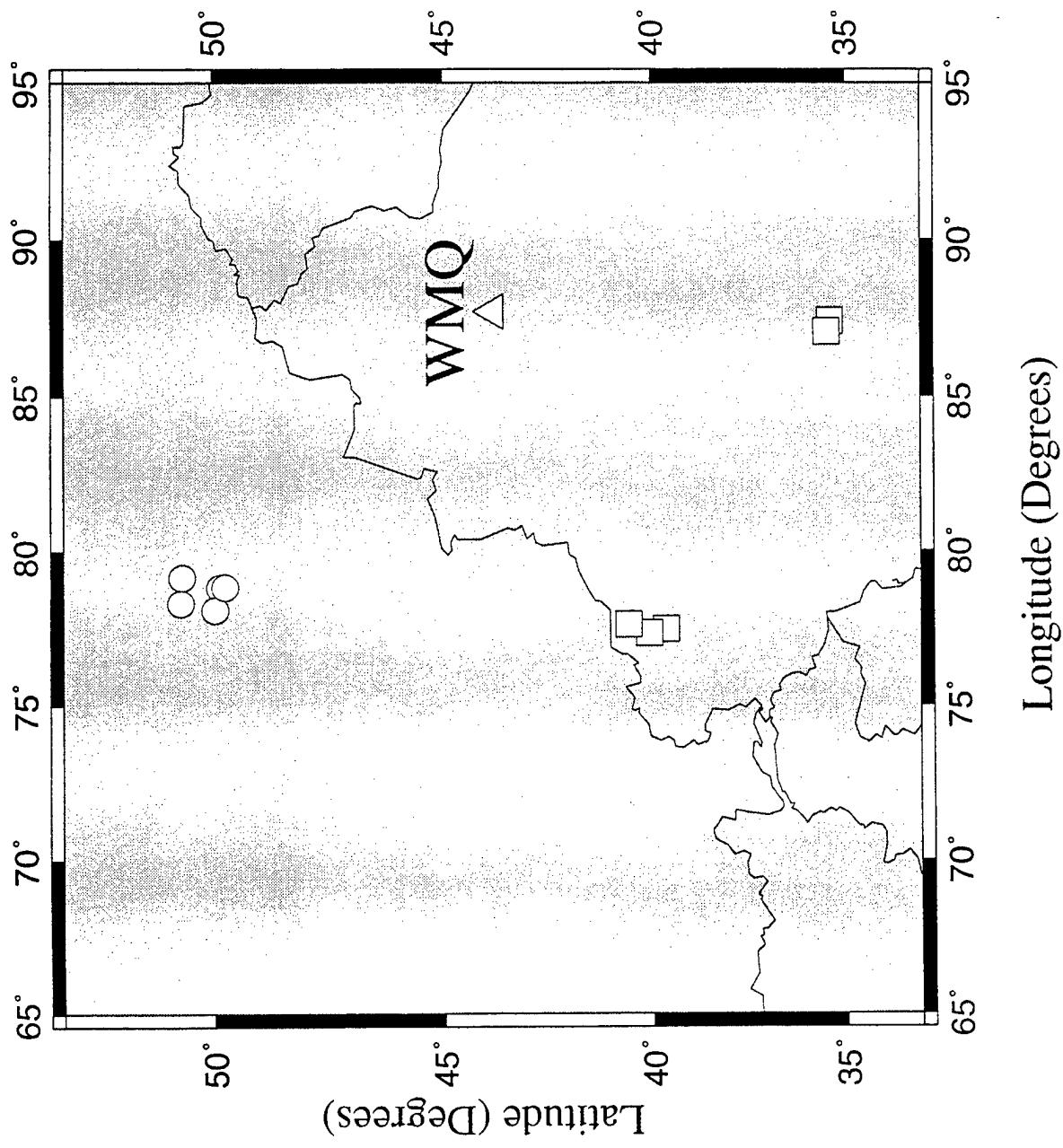


Figure 17. Map showing the locations of Soviet nuclear explosions and nearby earthquakes relative to station WMQ in China.

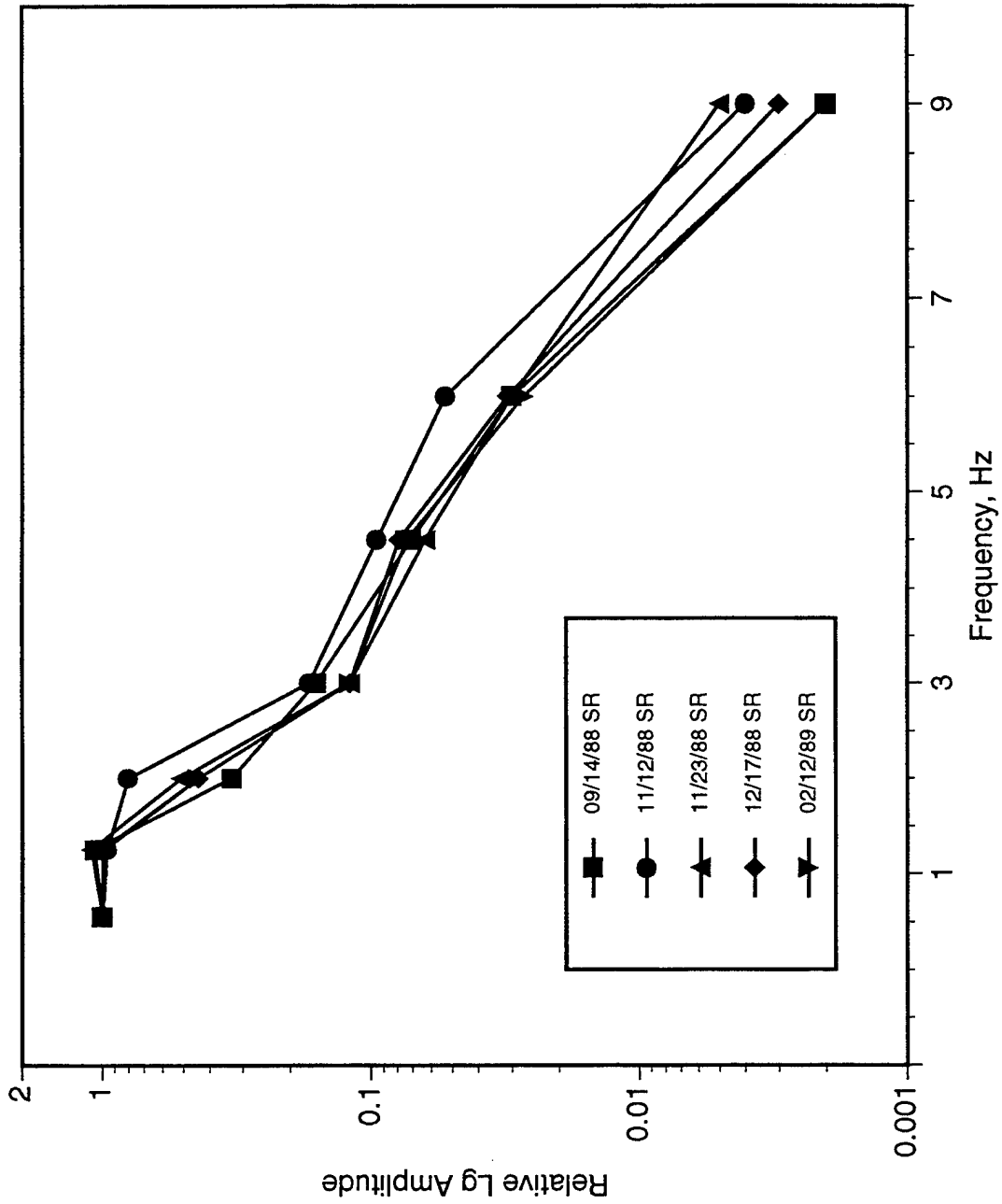


Figure 18. Relative Lg spectral estimates obtained for Shagan River nuclear explosions from traditional bandpass filter analyses of records at station WMQ using amplitudes measured in windows from 3.6 km/sec to 3 km/sec.

The relative spectral amplitudes for this longer window are shown in Figure 19. The scatter appears to be about the same and amplitudes again have maximum values near one at 0.55 Hz and 1.25 Hz and rapidly decline above 1.25 Hz. However, the decline toward higher frequencies is less rapid than for the shorter group velocity window. This difference appears to be related to including  $S_n$  and related high-frequency S phases which arrive with higher group velocities.

Figures 20 and 21 show the  $L_g$  spectral estimates for the two group velocity windows for five earthquakes recorded at WMQ at about the same epicentral distance as the Shagan River nuclear tests. The spectra for the earthquakes appear to show considerably more scatter between events, and the spectral differences appear to be dependent to some extent on propagation path. The three events west-southwest of WMQ (cf. Figure 16) show similar  $L_g$  spectral behavior, and the two events south of WMQ show similar behavior. For the events west-southwest of WMQ, the  $L_g$  spectral estimates show a gradual decline from maximum values of one near 0.55 Hz and 1.25 Hz to low values near 0.01 at 9 Hz. The two events from the south have  $L_g$  spectra which decline very rapidly over the interval 0.1 Hz to 3 Hz and then level off above that to values between 0.01 and 0.02 at high frequencies. The alternative group velocity windows don't seem to make much of a difference with regard to either spectral shape or scatter between events for these earthquakes; the propagation path appears to be a much stronger influence.

In Figure 22 we compare the average  $L_g$  spectral estimates observed at WMQ for the five Shagan River nuclear tests with the average spectra for the three earthquakes to the south-southwest and for the two earthquakes to the south at about the same distance. The average  $L_g$  spectral estimates for the earthquakes south-southwest of WMQ match closely the average explosion

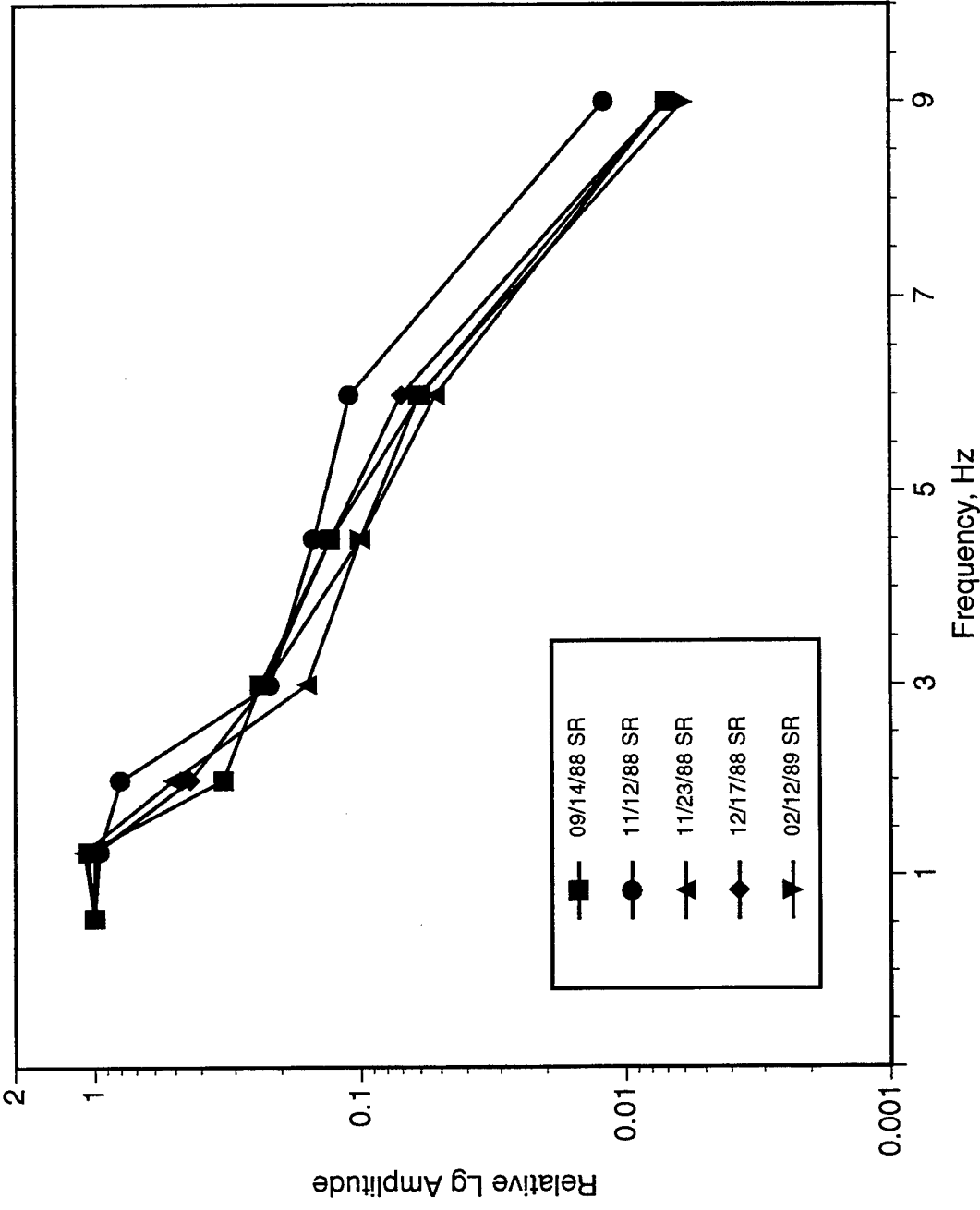


Figure 19. Relative Lg spectral estimates obtained for Shagan River nuclear explosions from traditional bandpass filter analyses of records at station WMQ using amplitudes measured in windows from 4.6 km/sec to 3 km/sec.

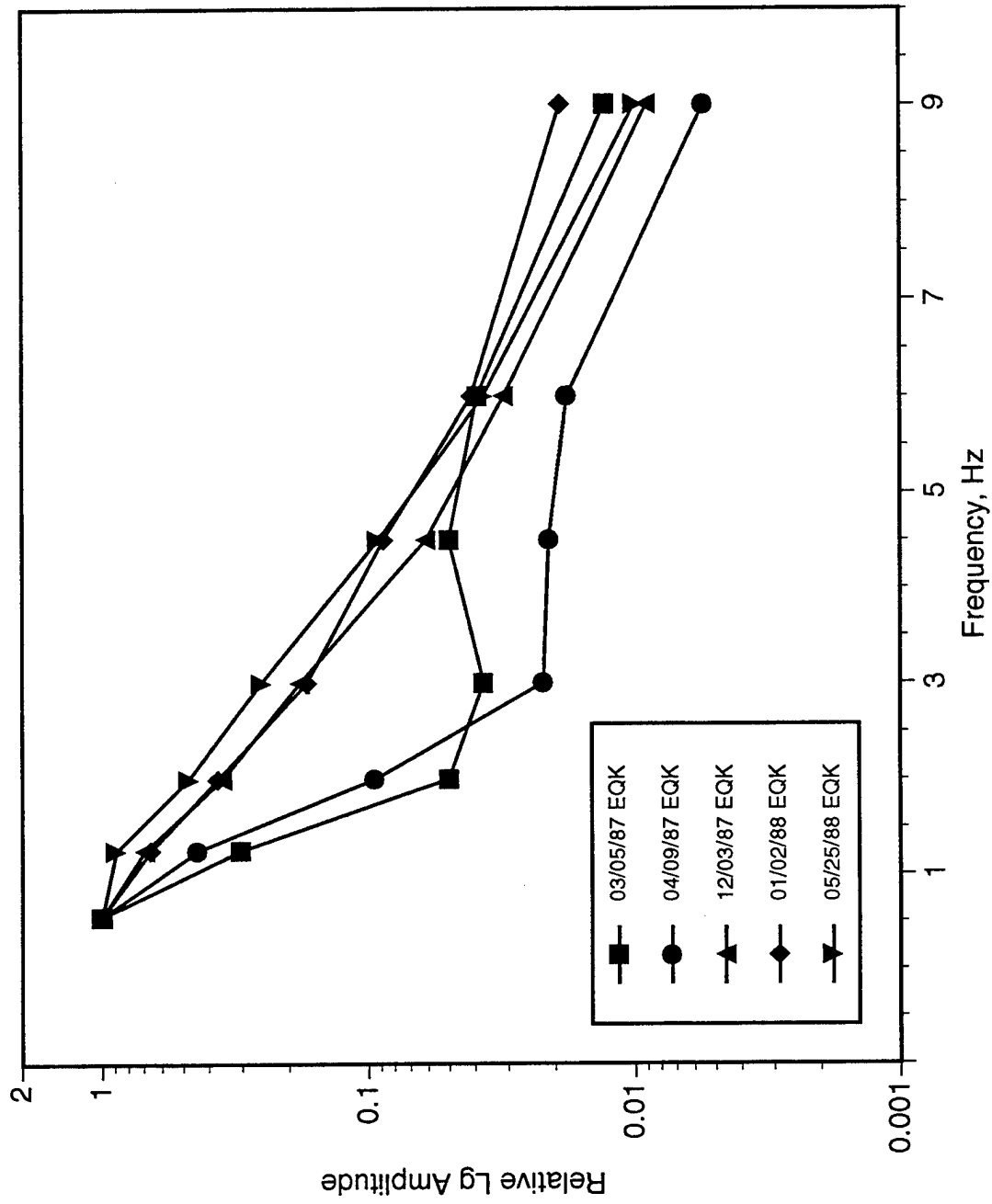


Figure 20. Relative Lg spectral estimates obtained for Asian earthquakes from traditional bandpass filter analyses of records at station WMQ at similar epicentral distances to the nuclear explosions at WMQ for measurements in window from 3.6 km/sec to 3 km/sec.

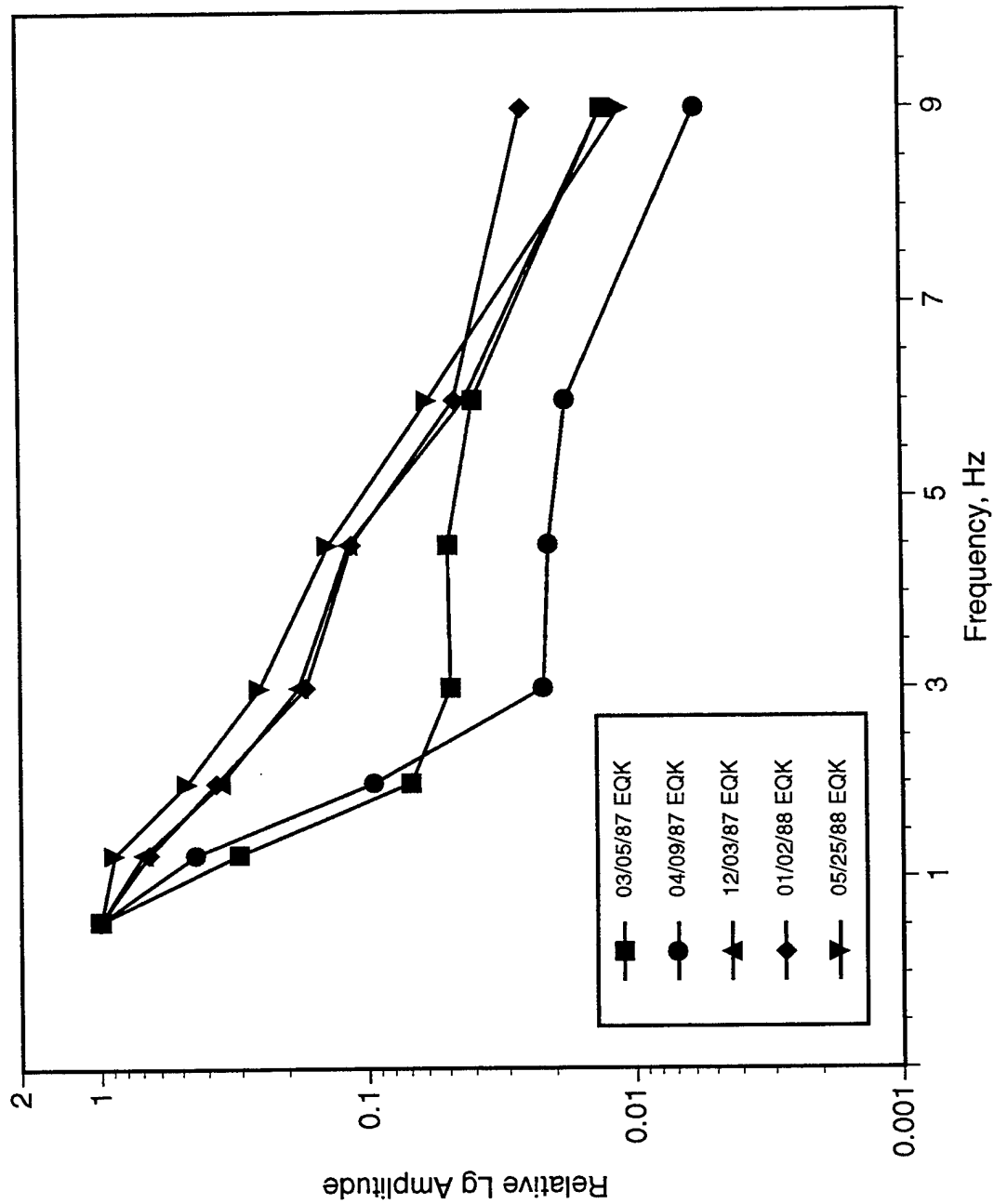


Figure 21. Relative Lg spectral estimates obtained for Asian earthquakes from traditional bandpass filter analyses of records at station WMQ at similar epicentral distances to the nuclear explosions at WMQ for measurements in window from 4.6 km/sec to 3 km/sec.

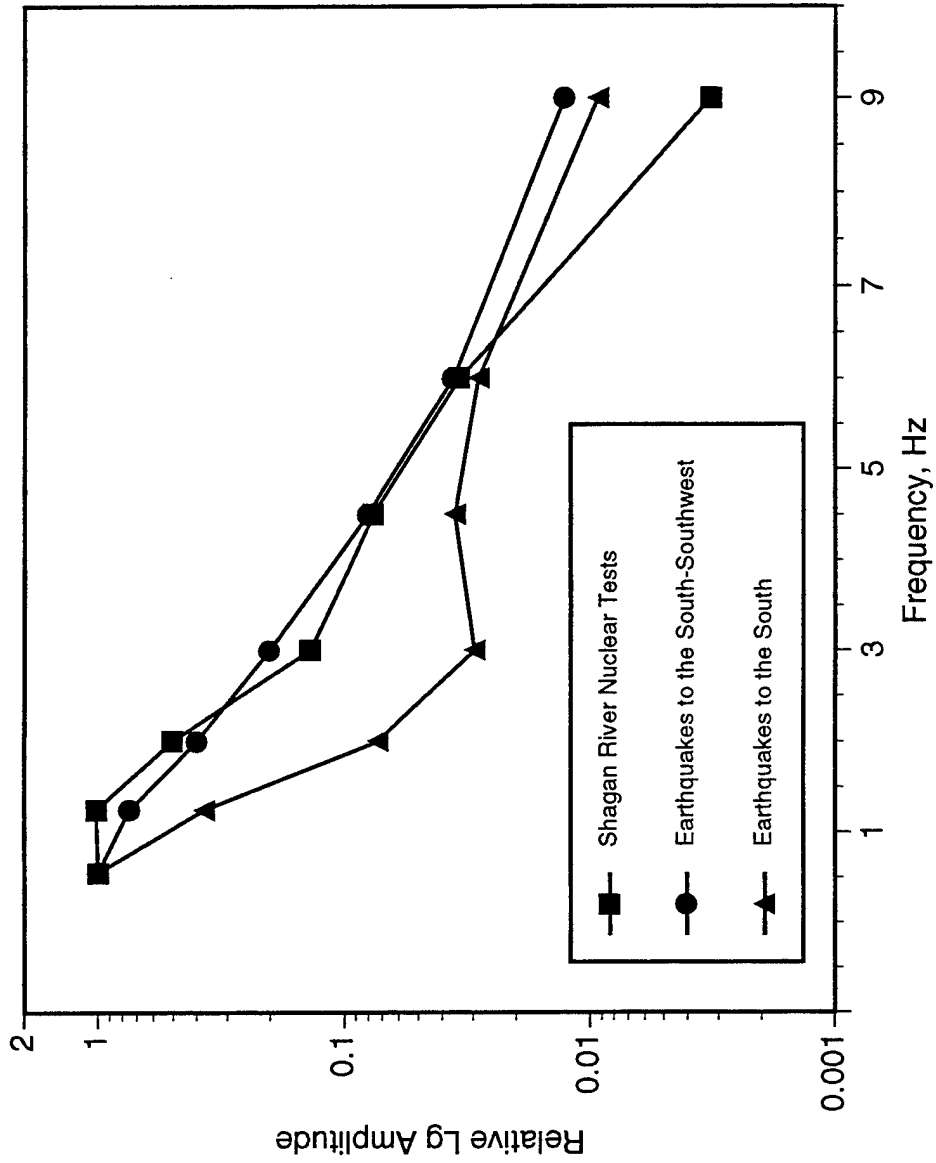


Figure 22. Comparison of average Lg spectral estimates for 5 Shagan River nuclear explosions recorded at station WMQ with average Lg spectra for 3 earthquakes to the south-southwest and for 2 earthquakes to the south at similar epicentral distances.

spectrum out to 6 Hz and then diverge and lie above the explosion spectrum by a factor of four at 9 Hz. The average  $L_g$  spectrum for the earthquakes south of WMQ lies well below (by as much as a factor of seven) the explosion spectrum over the frequency interval from 1.25 Hz to 4.5 Hz, but crosses and lies above the explosion spectrum by about a factor of three at 9 Hz.

Another factor which we have not explicitly accounted for in these comparisons for WMQ is the magnitude differences between the nuclear tests and the earthquakes. The average magnitude for the five nuclear tests which we analyzed from WMQ is 5.28  $m_b$ , and the average for the five earthquakes is 4.26  $m_b$ . As we saw above in Section 3, if the explosions are scaled down to the same magnitudes as the earthquakes, we would expect a significant increase in the high-frequency spectral amplitudes relative to low-frequency amplitudes for the explosions. Thus, when appropriately scaled, the relative  $L_g$  spectra for the nuclear explosions at WMQ should be richer in high frequencies than similar spectra for earthquakes recorded there at the same epicentral distance. This observation needs careful study with additional events because it implies that the behavior for the  $L_g$  spectra for these Asian explosions and earthquakes is quite different from that for western U.S. events.

#### **4.3 Application of Analyses to New Data from Soviet PNE's**

As noted above in Section 2, a database of regional recordings which recently became available for Asian nuclear explosions are the recordings at the Borovoye station (BRV) for Soviet PNE's. Although the epicentral distances to the events in this database cover a wide range (cf. Murphy et al., 1996), many of the event distances are far regional. We have focused our consideration of these data on the nearest PNE's to BRV. Figure 23 shows the locations of seven PNE explosions within 1000 km of BRV. One of the PNE's was fairly

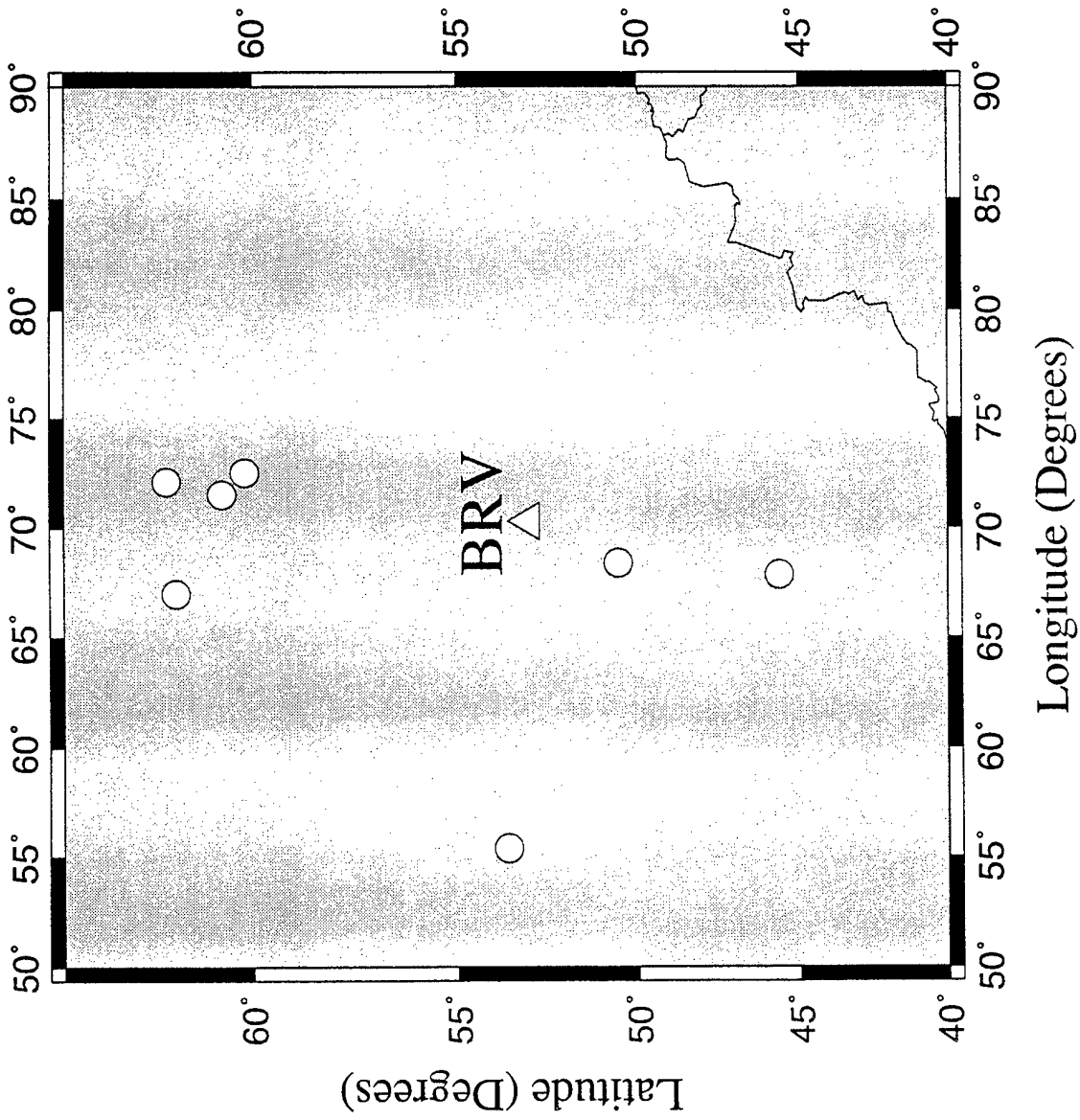


Figure 23. Map showing the locations of selected Soviet PNE explosions relative to station BRV.

close to BRV at a range of 311 km, while the other six events were at ranges from 801 km to 989 km. The region depicted is not known to contain major tectonic boundaries and is regarded as a stable continental platform region.

We applied the same bandpass filter analysis to the vertical-component records at station BRV from the PNE explosions. Figures 24 and 25 show examples of the bandpass filter results for a PNE to the north of BRV at a range of 980 km and another PNE to the south of BRV at a range of 925 km. Both records show clear initial P phases which become relatively more prominent in the higher frequency bands. These P signals appear fairly complex and have rather long duration; they are assumed to represent P-wave signals propagating in the upper mantle lid. At a somewhat later time (roughly 40 seconds after the initial P), another strong arrival is apparent on the record for the PNE to the north of BRV, but not on the record from the southern PNE. This phase is most prominent at frequencies from about 0.5 Hz to 3 Hz and arrives at a group velocity normally associated with Pg. The absence of this phase on the record for the southern PNE suggests some kind of propagation anomaly and the need for careful consideration of propagation influences on regional signals. Approximately 100 seconds after the initial P, a strong S<sub>n</sub> phase is apparent. This signal is strongest from the event to the north of BRV and appears more emergent from the event to the south, which again appears to indicate some propagation difference. L<sub>g</sub> is not prominent for the southern event where it arrives about 150 seconds after the initial P and is apparent mainly at lower frequencies (viz. 1 Hz to 3 Hz). L<sub>g</sub> for the event north of BRV has no clear initial arrival but appears rather as a coda phase which is again more prominent in the lower frequency bands.

We again used the band-pass filter results to obtain relative spectral amplitude estimates for the regional phases. Figure 26 shows L<sub>g</sub> spectral

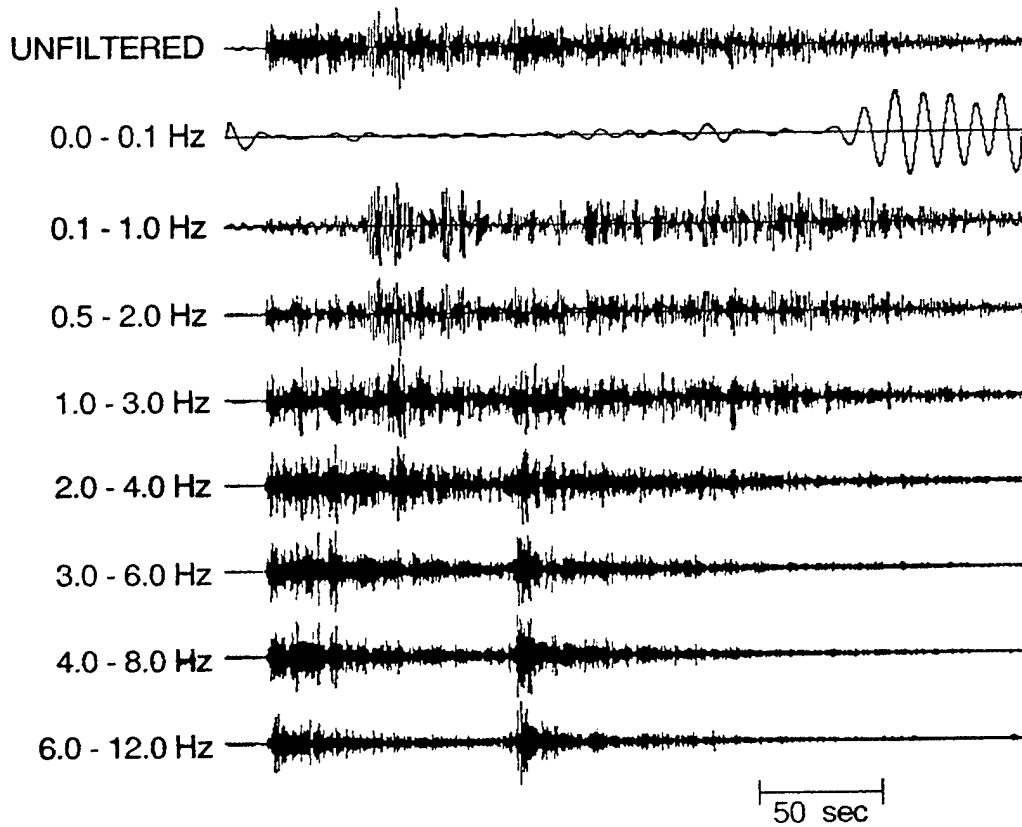


Figure 24. Traditional bandpass filter analysis of Soviet PNE explosion of December 10, 1980 recorded at station BRV (R = 980 km).

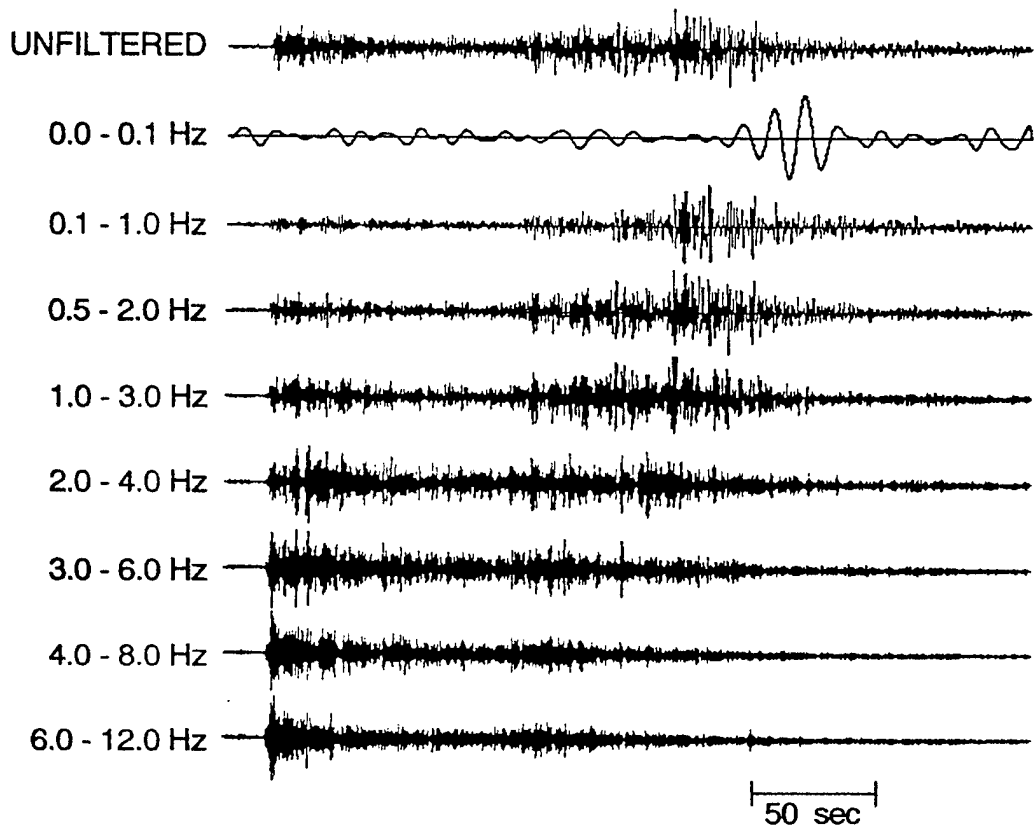


Figure 25. Traditional bandpass filter analysis of Soviet PNE explosion of October 26, 1980 recorded at station BRV ( $R = 925$  km).

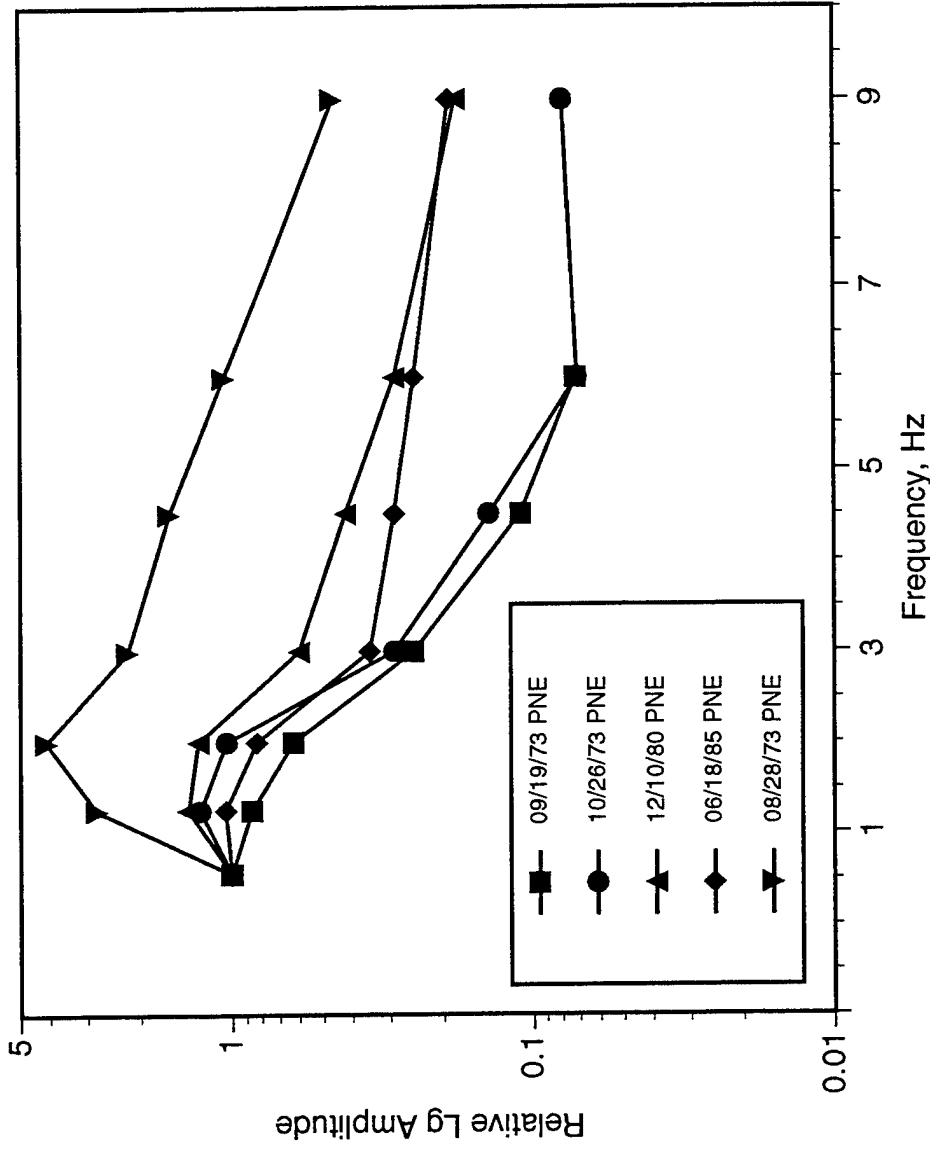


Figure 26. Relative Lg spectral estimates obtained for PNE explosions from traditional bandpass filter analyses of records at station BRV using amplitudes measured in window from 3.6 km/sec to 3 km/sec.

amplitudes measured in a group velocity window from 3.6 km/sec to 3.0 km/sec for five of the PNE's in Figure 23 recorded at BRV. The  $L_g$  spectrum for the explosion nearest to the station (viz. 08/28/73 PNE) is clearly different from the rest as it contains relatively more high-frequency than the other four events. This is probably related to proximity ( $R = 311$  km) of that event to the recording station with relatively low attenuation compared to the other four events which are located at larger epicentral distances (from 801 km to 979 km). The  $L_g$  spectral amplitudes in Figure 26 for the five PNE's reach their maximum values between 0.5 Hz and 2 Hz and then fall-off by factors between five and twenty toward high frequencies.

The  $L_g$  spectra in Figure 26 show considerable variability between events. Even if we consider only the spectra for the four events at about the same epicentral distance, we see differences which amount to only about a factor of two at frequencies less than 3 Hz but are up to a factor of four or more at higher frequencies. The instrument response at station BRV has varied somewhat with time. Because the events cover a time period of more than a decade, we thought that such instrument response changes could be a source for some of the observed variability between the spectral estimates. To account for this factor, we applied an approximate correction to the spectral amplitude estimates by dividing by the instrument gain at the filter center frequency for each filter. Figure 27 shows the relative  $L_g$  spectral estimates after applying this instrument response correction. Although the corrected spectral shapes are different than those seen in the previous figure, the correction to ground motion seems to have done little to reduce the variation between events. The revised  $L_g$  spectral estimates show a decline from maximum values near 0.55 Hz. The decline is rather slow for the near event but quite rapid for the four more distant PNE's. Although the  $L_g$  spectral estimates for the four distant events appear

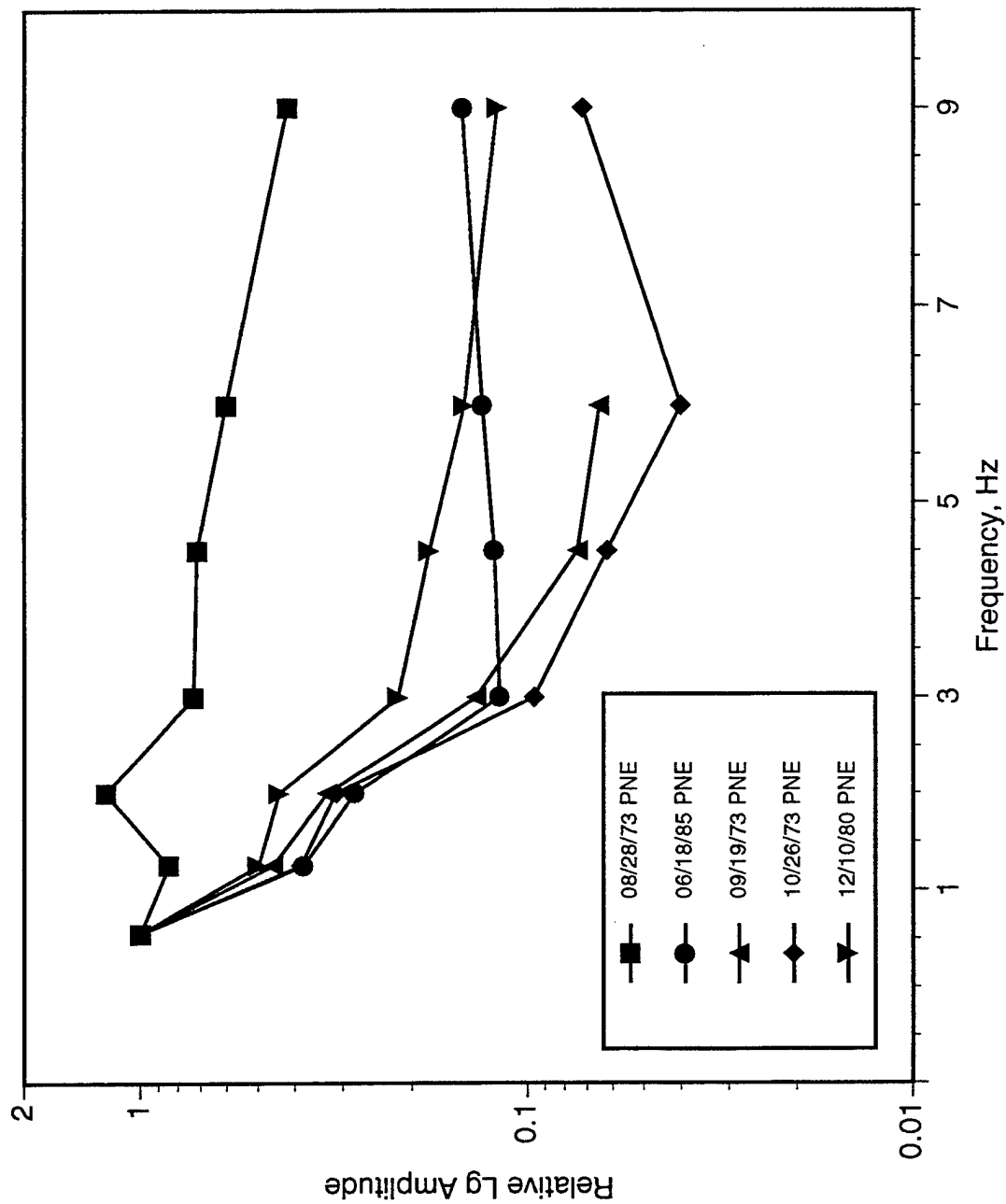


Figure 27. Relative Lg spectral estimates obtained for PNE explosions from traditional bandpass filter analyses of records at station BRV using amplitudes measured in window from 3.6 km/sec to 3 km/sec after adjustment for BRV instrument response.

fairly consistent at frequencies up to about 3 Hz, above 3 Hz the observations tend to diverge. At the high frequencies the  $L_g$  spectral estimates for the two events north of BRV (viz. 06/18/85 and 12/10/80 PNE's) tend to have values a factor of two to four larger than those for the events to the south (viz. 09/19/73 PNE) and to the west (viz. 10/26/73 PNE). Since these differences in the  $L_g$  spectra at high frequencies do not appear to be related to the instrument response variations at BRV, it seems most likely that they are associated with either  $L_g$  propagation variation in the region surrounding BRV or possibly differences in the source excitation between events. In our continuing research we will investigate further these factors for the PNE's observed at BRV as well as for the events in other source regions.

## 5. Summary and Conclusions

### 5.1 Review of Procedures

We have reviewed the available regional seismic data from digital stations for underground nuclear explosion tests and comparable earthquakes. From the available data we have selected a representative sample of regional waveforms for events from the western U.S. and Eurasia. The selected waveforms for western U.S. explosions at NTS come from several different stations and cover epicentral distances from 220 km to 1450 km, and the comparable earthquakes are at distances from 160 km to 1670 km. The western U.S. events have magnitudes between 2.9  $m_b$  and 6.2  $m_b$ . The Eurasian nuclear explosions in the database come from three regular test sites (viz. Shagan River in East Kazakhstan, Novaya Zemlya in Russia, and Lop Nor in western China) and PNE explosions throughout the former Soviet Union. The regional stations currently in the database for the Eurasian events include several digital stations from within the former Soviet Union, selected CDSN stations in China, and the northern European/Scandinavian regional array stations. The selected waveforms for the Eurasian nuclear explosions cover epicentral distances from 310 km to 4030 km, and the comparable earthquakes are at distances from 130 km to 4220 km. The Eurasian events have magnitudes between 3.8  $m_b$  and 6.4  $m_b$ .

Our objective in this research is to use these data to investigate the transportability of regional phase spectral ratio discriminants. In particular, we have been attempting to identify algorithms for measuring regional phase spectral ratios which can be easily applied to a variety of regional phases and which will provide an effective discriminant measure in a variety of different source/propagation environments. Our studies have focused mainly on utilization of some alternative bandpass filtering schemes to extract spectral

estimates from the regional phases. In addition, we have been analyzing transportability and measurement issues associated with source size and attenuation. For the former we have used theoretical source scaling procedures to compare relative spectral ratios for nuclear explosions and earthquakes of equivalent magnitudes and to investigate how such source size differences might affect the spectral ratio measurements. With regard to regional phase attenuation, we have conducted work to identify published reports on regional phase propagation in many different regions, and we are working toward models to account for the effects of attenuation differences on various regional phases.

## **5.2 Summary of Main Findings**

Although this research program has not yet evolved to the stage where we can provide final conclusions and procedures for transporting regional phase spectral ratio discriminant measures, several of the observations described in previous sections appear to lead to conclusions which impact on transportability of potential regional phase discriminants and, in particular, on spectral ratio discriminants. First, the original  $L_g$  spectral discriminant was based on observations at nearer regional distances from events in the western U.S. Most regional observations from Eurasian nuclear explosions are at considerably farther distances, so regional phase spectral shapes are not directly comparable. Second, spectral estimates derived from bandpass filters show regional phase spectral differences between NTS nuclear tests and nearby earthquakes similar to those seen in previous investigations; the broader filters tend to be smoother and show the differences between source types at lower frequencies probably because they tend to average in energy from higher-frequency bands. Third, the original  $L_g$  spectral ratio discriminant

was based on comparisons of NTS nuclear explosions and earthquakes from the surrounding area; and most of the nuclear explosions have larger magnitudes than the earthquakes near NTS which are available for comparison. Scaling the explosions down to be equivalent to the earthquakes tends to reduce, but not eliminate,  $L_g$  spectral differences between the source types which have been observed at some regional stations. Observed regional P spectral differences tend to be smaller and may be eliminated when the events are scaled. Fourth, differences in  $L_g/P$  ratios as a function of frequency for Eurasian nuclear explosions and earthquakes implies differences in individual regional phase spectra, but we do not see  $L_g$  spectral behavior in the far-regional Eurasian observations like that in the western U.S. In fact, after scaling to similar magnitude levels, the  $L_g$  spectra for Eurasian nuclear tests would probably show the opposite tendency - i.e.  $L_g$  for the scaled nuclear tests relatively richer in high frequencies than for earthquakes. Attenuation differences for the propagation paths from the explosion and earthquake source areas could be the cause, but this result could also imply a fundamental difference in the way  $L_g$  is generated by explosions in the two different source environments, which would certainly affect discriminant transportability between the regions.

### **5.3 Plans for Future Work**

Several issues remain to be resolved to bring this research program to successful conclusion. Two of the most critical elements are (1) deciding on the algorithm to use for determining the spectral ratio measurements from the signal waveforms and (2) defining the procedure to correct for signal attenuation in different regions. In our initial work we have tried a few alternative spectral estimation schemes; we plan to test one or two additional variations and

compare results with Fourier spectral estimates. With regard to attenuation we plan to rely primarily on published results from previous studies for defining a frequency-dependent correction for each region which will normalize the spectrum to a fixed distance range. Q models to describe  $L_G$  attenuation are currently available for many different regions of the world, and we have collected much of this information already; but descriptions of regional P-wave propagation may be more problematic. We will seek to identify published results or analyze the signals available in the regional database to help resolve the P-wave attenuation. Another element which needs further attention is instrument response; such corrections have not always been necessary in our prior analyses because we have been comparing observations from common or similar recording instruments. As we attempt to make the measurement and procedures more general, corrections to the spectral measurements for the instrument will be determined and applied using known instrument response characteristics for the recording systems. Finally, some of our preliminary results seem to suggest that  $L_G$  signal excitation from explosion sources may vary between regions; this is potentially very important to the concept of transportability. We will seek to resolve this issue with additional empirical studies and drawing upon findings from theoretical investigations of the relative excitation of regional phases in different source environments which are being conducted under a separate project.

## 6. References

- Baumgardt, D. R., and G. B. Young (1990). "Regional Seismic Waveform Discriminants and Case-Based Event Identification Using Regional Arrays," *Bull. Seism. Soc. Am.*, 80, pp. 1874 - 1892.
- Bennett, T. J., and J. R. Murphy (1986). "Analysis of Seismic Discrimination Capabilities Using Regional Data from Western United States Events," *Bull. Seism. Soc. Am.*, 76, pp. 1069 -1086.
- Bennett, T. J., B. W. Barker, K. L. McLaughlin, and J. R. Murphy (1989). "Regional Discrimination of Quarry Blasts, Earthquakes and Underground Nuclear Explosions," GL-TR-89-0114, ADA223148.
- Bennett, T. J., A. K. Campanella, J. F. Scheimer, and J. R. Murphy (1992). "Demonstration of Regional Discrimination of Eurasian Seismic Events Using Observations at Soviet IRIS and CDSN Stations," PL-TR-92-2090, ADA253275.
- Bennett, T. J., M. E. Marshall, B. W. Barker, and J. R. Murphy (1994). "Characteristics of Rockbursts for Use in Seismic Discrimination," PL-TR-94-2269, ADA290881.
- Bennett, T. J., B. W. Barker, M. E. Marshall, and J. R. Murphy (1995). "Detection and Identification of Small Regional Seismic Events," PL-TR-95-2125, ADA305536.
- Bennett, T. J., M. E. Marshall, B. W. Barker, K. L. McLaughlin, and J. R. Murphy (1996). "Investigations of the Seismic Discrimination of Rockbursts," PL-TR-96-2184.
- Blandford, R. (1981). "Seismic Discrimination Problems at Regional Distances," in *Identification of Seismic Source -Earthquake or Underground Explosion*, D. Reidel Publishing Co., pp. 695-740.
- Chael, E. P. (1991). "Effects of Explosion Source Parameters on High-Frequency Pg Spectra," in *Explosion Source Phenomenology*, Geophysical Monograph 65, American Geophysical Union, pp. 211 - 217.
- Dysart, P. S., and J. J. Pulli (1990). "Regional Seismic Event Classification at the NORESS Array: Seismological Measurements and the Use of Trained Neural Networks," *Bull. Seism. Soc. Am.*, 80, pp. 1910 - 1933.
- Jih, R.-S., and C. S. Lynnes (1992). "Studies of Regional Phase Propagation in Eurasia," PL-TR-93-2003, ADA262801.
- Kadinsky-Cade, K., M. Barazangi, J. Oliver, and B. Isacks (1981). "Lateral Variations of High-Frequency Wave Propagation at Regional Distances Across the Turkish-Iranian Plateaus," *J. Geophys. Res.*, 86, pp. 9377 - 9396.

- Mueller, R. A., and J. R. Murphy (1971). "Seismic Characteristics of Underground Nuclear Detonations. Part I. Seismic Spectrum Scaling," Bull. Seism. Soc. Am., 61, pp. 1675 - 1692.
- Murphy, J. R. (1977). "Seismic Source Functions and Magnitude Determinations for Underground Nuclear Detonations," Bull. Seism. Soc. Am., 67, pp. 135 - 158.
- Murphy, J. R., and T. J. Bennett (1982). "A Discrimination Analysis of Short-Period Regional Seismic Data Recorded at Tonto Forest Observatory," Bull. Seism. Soc. Am., 72, pp. 1351 - 1366.
- Murphy, J. R., M. E. Marshall, B. W. Barker, T. J. Bennett, L. T. Grant, and I. N. Gupta (1995). "Calibration of Local Magnitude Scales for Use in Seismic Monitoring," PL-TR-95-2105, ADA304034.
- Murphy, J. R., D. D. Sultanov, B. W. Barker, I. O. Kitov, and M. E. Marshall (1996). "Regional Seismic Detection Analyses of Selected Soviet Peaceful Nuclear Explosions," SSS-DFR-96-15503.
- Nersesov, I. L., and T. G. Rautian (1964). "Kinematics and Dynamics of Seismic Waves to Distances of 3500 km from the Epicenter," Akad. Nauk SSSR, Trudy Inst. Fiziki. Zemli, 32, pp. 63 - 87.
- Nuttli, O. W. (1981). "On Attenuation of Lg Waves in Western and Central Asia and Their Use as a Discriminant Between Earthquakes and Explosions," Bull. Seism. Soc. Am., 71, pp. 249 - 261.
- Piwinskii, A. J., and D. L. Springer (1978). "Propagation of Lg Waves Across Eastern Europe and Asia," LLNL Report UCRL-52494.
- Pomeroy, P. W., W. J. Best, and T. V. McEvelly (1982). "Test Ban Treaty Verification with Regional Data - A Review," Bull. Seism. Soc. Am., 72, pp. S89 - S129.
- Ryall, A. (1970). "Seismic Identification at Short Distances," in Copies of Papers Presented at Wood's Hole Conference on Seismic Discrimination, 2, DARPA, Arlington, VA.
- Taylor, S. R. (1991). "Regional Seismic Observations from NTS Explosions," in Explosion Source Phenomenology, Geophysical Monograph 65, American Geophysical Union, pp. 185 - 196.
- Taylor, S. R., N. W. Sherman, and M. D. Denny (1988). "Spectral Discrimination Between NTS Explosions and Western United States Earthquakes at Regional Distances," Bull. Seism. Soc. Am., 78, pp. 1563 - 1579.

- Taylor, S. R., M. D. Denny, E. S. Vergino, and R. E. Glaser (1989). "Regional Discrimination Between NTS Explosions and Western U. S. Earthquakes," *Bull. Seism. Soc. Am.*, 78, pp. 1142 - 1176.
- von Seggern, D., and R. Blandford (1972). "Source Time Functions and Spectra for Underground Nuclear Explosions," *Geophys. J.*, 31, pp. 83 - 97.
- Walter, W. R., and K. F. Priestley (1991). "High-Frequency P Wave Spectra from Explosions and Earthquakes," in *Explosion Source Phenomenology*, Geophysical Monograph 65, American Geophysical Union, pp. 219 - 228.
- Xie, J.-K., and B. J. Mitchell (1990). "Lg Coda Q Variations Across Eurasia," in *Papers Presented at 12th Annual DARPA/GL Seismic Research Symposium*, GL-TR-90-0212, ADA226635.

THOMAS AHRENS  
SEISMOLOGICAL LABORATORY 252-21  
CALIFORNIA INSTITUTE OF TECHNOLOGY  
PASADENA, CA 91125

SHELTON ALEXANDER  
PENNSYLVANIA STATE UNIVERSITY  
DEPARTMENT OF GEOSCIENCES  
537 DEIKE BUILDING  
UNIVERSITY PARK, PA 16801

RICHARD BARDZELL  
ACIS  
DCI/ACIS  
WASHINGTON, DC 20505

DOUGLAS BAUMGARDT  
ENSCO INC.  
5400 PORT ROYAL ROAD  
SPRINGFIELD, VA 22151

WILLIAM BENSON  
NAS/COS  
ROOM HA372  
2001 WISCONSIN AVE. NW  
WASHINGTON, DC 20007

ROBERT BLANDFORD  
AFTAC  
1300 N. 17TH STREET  
SUITE 1450  
ARLINGTON, VA 22209-2308

RHETT BUTLER  
IRIS  
1200 NEW YORK AVE., NW  
SUITE 800  
WASHINGTON, DC 20005

CATHERINE DE GROOT-HEDLIN  
UNIVERSITY OF CALIFORNIA, SAN DIEGO  
INSTITUTE OF GEOPHYSICS AND PLANETARY PHYSICS  
8604 LA JOLLA SHORES DRIVE  
SAN DIEGO, CA 92093

SEAN DORAN  
ACIS  
DCI/ACIS  
WASHINGTON, DC 20505

RICHARD J. FANTEL  
BUREAU OF MINES  
DEPT OF INTERIOR, BLDG 20  
DENVER FEDERAL CENTER  
DENVER, CO 80225

RALPH ALEWINE  
NTPO  
1901 N. MOORE STREET, SUITE 609  
ARLINGTON, VA 22209

MUA WIA BARAZANGI  
INSTITUTE FOR THE STUDY OF THE CONTINENTS  
3126 SNEE HALL  
CORNELL UNIVERSITY  
ITHACA, NY 14853

T.G. BARKER  
MAXWELL TECHNOLOGIES  
P.O. BOX 23558  
SAN DIEGO, CA 92123

THERON J. BENNETT  
MAXWELL TECHNOLOGIES  
11800 SUNRISE VALLEY DRIVE SUITE 1212  
RESTON, VA 22091

JONATHAN BERGER  
UNIVERSITY OF CA, SAN DIEGO  
SCRIPPS INSTITUTION OF OCEANOGRAPHY IGPP, 0225  
9500 GILMAN DRIVE  
LA JOLLA, CA 92093-0225

STEVEN BRATT  
NTPO  
1901 N. MOORE STREET, SUITE 609  
ARLINGTON, VA 22209

LESLIE A. CASEY  
DOE  
1000 INDEPENDENCE AVE. SW  
NN-20  
WASHINGTON, DC 20585-0420

STANLEY DICKINSON  
AFOSR  
110 DUNCAN AVENUE, SUITE B115  
BOLLING AFB  
WASHINGTON, D.C. 20332-001

DIANE I. DOSER  
DEPARTMENT OF GEOLOGICAL SCIENCES  
THE UNIVERSITY OF TEXAS AT EL PASO  
EL PASO, TX 79968

JOHN FILSON  
ACIS/TMG/NTT  
ROOM 6T11 NHB  
WASHINGTON, DC 20505

MARK D. FISK  
MISSION RESEARCH CORPORATION  
735 STATE STREET  
P.O. DRAWER 719  
SANTA BARBARA, CA 93102-0719

LORI GRANT  
MULTIMAX, INC.  
311C FOREST AVE. SUITE 3  
PACIFIC GROVE, CA 93950

I. N. GUPTA  
MULTIMAX, INC.  
1441 MCCORMICK DRIVE  
LARGO, MD 20774

JAMES HAYES  
NSF  
4201 WILSON BLVD., ROOM 785  
ARLINGTON, VA 22230

MICHAEL HEDLIN  
UNIVERSITY OF CALIFORNIA, SAN DIEGO  
SCRIPPS INSTITUTION OF OCEANOGRAPHY IGPP, 0225  
9500 GILMAN DRIVE  
LA JOLLA, CA 92093-0225

EUGENE HERRIN  
SOUTHERN METHODIST UNIVERSITY  
DEPARTMENT OF GEOLOGICAL SCIENCES  
DALLAS, TX 75275-0395

VINDELL HSU  
HQ/AFTAC/TTR  
1030 S. HIGHWAY A1A  
PATRICK AFB, FL 32925-3002

RONG-SONG JIH  
PHILLIPS LABORATORY  
EARTH SCIENCES DIVISION  
29 RANDOLPH ROAD  
HANSCOM AFB, MA 01731-3010

LAWRENCE LIVERMORE NATIONAL LABORATORY  
ATTN: TECHNICAL STAFF (PLS ROUTE)  
PO BOX 808, MS L-200  
LIVERMORE, CA 94551

LAWRENCE LIVERMORE NATIONAL LABORATORY  
ATTN: TECHNICAL STAFF (PLS ROUTE)  
PO BOX 808, MS L-221  
LIVERMORE, CA 94551

ROBERT GEIL  
DOE  
PALAIS DES NATIONS, RM D615  
GENEVA 10, SWITZERLAND

HENRY GRAY  
SMU STATISTICS DEPARTMENT  
P.O. BOX 750302  
DALLAS, TX 75275-0302

DAVID HARKRIDER  
PHILLIPS LABORATORY  
EARTH SCIENCES DIVISION  
29 RANDOLPH ROAD  
HANSCOM AFB, MA 01731-3010

THOMAS HEARN  
NEW MEXICO STATE UNIVERSITY  
DEPARTMENT OF PHYSICS  
LAS CRUCES, NM 88003

DONALD HELMBERGER  
CALIFORNIA INSTITUTE OF TECHNOLOGY  
DIVISION OF GEOLOGICAL & PLANETARY SCIENCES  
SEISMOLOGICAL LABORATORY  
PASADENA, CA 91125

ROBERT HERRMANN  
ST. LOUIS UNIVERSITY  
DEPARTMENT OF EARTH & ATMOSPHERIC SCIENCES  
3507 LACLEDE AVENUE  
ST. LOUIS, MO 63103

ANTHONY IANNACCHIONE  
BUREAU OF MINES  
COCHRANE MILL ROAD  
PO BOX 18070  
PITTSBURGH, PA 15236-9986

THOMAS JORDAN  
MASSACHUSETTS INSTITUTE OF TECHNOLOGY  
EARTH, ATMOSPHERIC & PLANETARY SCIENCES  
77 MASSACHUSETTS AVENUE, 54-918  
CAMBRIDGE, MA 02139

LAWRENCE LIVERMORE NATIONAL LABORATORY  
ATTN: TECHNICAL STAFF (PLS ROUTE)  
PO BOX 808, MS L-207  
LIVERMORE, CA 94551

LAWRENCE LIVERMORE NATIONAL LABORATORY  
ATTN: TECHNICAL STAFF (PLS ROUTE)  
LLNL  
PO BOX 808, MS L-175  
LIVERMORE, CA 94551

LAWRENCE LIVERMORE NATIONAL LABORATORY  
ATTN: TECHNICAL STAFF (PLS ROUTE)  
PO BOX 808, MS L-208  
LIVERMORE, CA 94551

LAWRENCE LIVERMORE NATIONAL LABORATORY  
ATTN: TECHNICAL STAFF (PLS ROUTE)  
PO BOX 808, MS L-202  
LIVERMORE, CA 94551

LAWRENCE LIVERMORE NATIONAL LABORATORY  
ATTN: TECHNICAL STAFF (PLS ROUTE)  
PO BOX 808, MS L-195  
LIVERMORE, CA 94551

LAWRENCE LIVERMORE NATIONAL LABORATORY  
ATTN: TECHNICAL STAFF (PLS ROUTE)  
PO BOX 808, MS L-205  
LIVERMORE, CA 94551

THORNE LAY  
UNIVERSITY OF CALIFORNIA, SANTA CRUZ  
EARTH SCIENCES DEPARTMENT  
EARTH & MARINE SCIENCE BUILDING  
SANTA CRUZ, CA 95064

ANATOLI L. LEVSHIN  
DEPARTMENT OF PHYSICS  
UNIVERSITY OF COLORADO  
CAMPUS BOX 390  
BOULDER, CO 80309-0309

DONALD A. LINGER  
DNA  
6801 TELEGRAPH ROAD  
ALEXANDRIA, VA 22310

LOS ALAMOS NATIONAL LABORATORY  
ATTN: TECHNICAL STAFF (PLS ROUTE)  
PO BOX 1663, MS F659  
LOS ALAMOS, NM 87545

LOS ALAMOS NATIONAL LABORATORY  
ATTN: TECHNICAL STAFF (PLS ROUTE)  
PO BOX 1663, MS F665  
LOS ALAMOS, NM 87545

LOS ALAMOS NATIONAL LABORATORY  
ATTN: TECHNICAL STAFF (PLS ROUTE)  
PO BOX 1663, MS D460  
LOS ALAMOS, NM 87545

LOS ALAMOS NATIONAL LABORATORY  
ATTN: TECHNICAL STAFF (PLS ROUTE)  
PO BOX 1663, MS C335  
LOS ALAMOS, NM 87545

GARY MCCARTOR  
SOUTHERN METHODIST UNIVERSITY  
DEPARTMENT OF PHYSICS  
DALLAS, TX 75275-0395

KEITH MCLAUGHLIN  
MAXWELL TECHNOLOGIES  
P.O. BOX 23558  
SAN DIEGO, CA 92123

BRIAN MITCHELL  
DEPARTMENT OF EARTH & ATMOSPHERIC SCIENCES  
ST. LOUIS UNIVERSITY  
3507 LACLEDE AVENUE  
ST. LOUIS, MO 63103

RICHARD MORROW  
USACDA/IVI  
320 21ST STREET, N.W.  
WASHINGTON, DC 20451

JOHN MURPHY  
MAXWELL TECHNOLOGIES  
11800 SUNRISE VALLEY DRIVE SUITE 1212  
RESTON, VA 22091

JAMES NI  
NEW MEXICO STATE UNIVERSITY  
DEPARTMENT OF PHYSICS  
LAS CRUCES, NM 88003

JOHN ORCUTT  
INSTITUTE OF GEOPHYSICS AND PLANETARY PHYSICS  
UNIVERSITY OF CALIFORNIA, SAN DIEGO  
LA JOLLA, CA 92093

PACIFIC NORTHWEST NATIONAL LABORATORY  
ATTN: TECHNICAL STAFF (PLS ROUTE)  
PO BOX 999, MS K6-48  
RICHLAND, WA 99352

PACIFIC NORTHWEST NATIONAL LABORATORY  
ATTN: TECHNICAL STAFF (PLS ROUTE)  
PO BOX 999, MS K7-34  
RICHLAND, WA 99352

PACIFIC NORTHWEST NATIONAL LABORATORY  
ATTN: TECHNICAL STAFF (PLS ROUTE)  
PO BOX 999, MS K6-40  
RICHLAND, WA 99352

PACIFIC NORTHWEST NATIONAL LABORATORY  
ATTN: TECHNICAL STAFF (PLS ROUTE)  
PO BOX 999, MS K6-84  
RICHLAND, WA 99352

PACIFIC NORTHWEST NATIONAL LABORATORY  
ATTN: TECHNICAL STAFF (PLS ROUTE)  
PO BOX 999, MS K5-12  
RICHLAND, WA 99352

FRANK PILOTTE  
HQ/AFTAC/TT  
1030 S. HIGHWAY A1A  
PATRICK AFB, FL 32925-3002

KEITH PRIESTLEY  
DEPARTMENT OF EARTH SCIENCES  
UNIVERSITY OF CAMBRIDGE  
MADINGLEY RISE, MADINGLEY ROAD  
CAMBRIDGE, CB3 0EZ UK

JAY PULLI  
BBN  
1300 NORTH 17TH STREET  
ROSSLYN, VA 22209

PAUL RICHARDS  
COLUMBIA UNIVERSITY  
LAMONT-DOHERTY EARTH OBSERVATORY  
PALISADES, NY 10964

DAVID RUSSELL  
HQ AFTAC/TTR  
1030 SOUTH HIGHWAY A1A  
PATRICK AFB, FL 32925-3002

CHANDAN SAIKIA  
WOODWARD-CLYDE FEDERAL SERVICES  
566 EL DORADO ST., SUITE 100  
PASADENA, CA 91101-2560

SANDIA NATIONAL LABORATORY  
ATTN: TECHNICAL STAFF (PLS ROUTE)  
DEPT. 5704  
MS 0979, PO BOX 5800  
ALBUQUERQUE, NM 87185-0979

SANDIA NATIONAL LABORATORY  
ATTN: TECHNICAL STAFF (PLS ROUTE)  
DEPT. 5791  
MS 0567, PO BOX 5800  
ALBUQUERQUE, NM 87185-0567

SANDIA NATIONAL LABORATORY  
ATTN: TECHNICAL STAFF (PLS ROUTE)  
DEPT. 9311  
MS 1159, PO BOX 5800  
ALBUQUERQUE, NM 87185-1159

SANDIA NATIONAL LABORATORY  
ATTN: TECHNICAL STAFF (PLS ROUTE)  
DEPT. 5704  
MS 0655, PO BOX 5800  
ALBUQUERQUE, NM 87185-0655

SANDIA NATIONAL LABORATORY  
ATTN: TECHNICAL STAFF (PLS ROUTE)  
DEPT. 5736  
MS 0655, PO BOX 5800  
ALBUQUERQUE, NM 87185-0655

THOMAS SERENO JR.  
SCIENCE APPLICATIONS INTERNATIONAL  
CORPORATION  
10260 CAMPUS POINT DRIVE  
SAN DIEGO, CA 92121

AVI SHAPIRA  
SEISMOLOGY DIVISION  
THE INSTITUTE FOR PETROLEUM RESEARCH AND  
GEOPHYSICS  
P.O.B. 2286, NOLON 58122 ISRAEL

ROBERT SHUMWAY  
410 MRAK HALL  
DIVISION OF STATISTICS  
UNIVERSITY OF CALIFORNIA  
DAVIS, CA 95616-8671

MATTHEW SIBOL  
ENSCO, INC.  
445 PINEDA COURT  
MELBOURNE, FL 32940

DAVID SIMPSON  
IRIS  
1200 NEW YORK AVE., NW  
SUITE 800  
WASHINGTON, DC 20005

JEFFRY STEVENS  
MAXWELL TECHNOLOGIES  
P.O. BOX 23558  
SAN DIEGO, CA 92123

BRIAN SULLIVAN  
BOSTON COLLEGE  
INSITUTE FOR SPACE RESEARCH  
140 COMMONWEALTH AVENUE  
CHESTNUT HILL, MA 02167

NAFI TOKSOZ  
EARTH RESOURCES LABORATORY, M.I.T.  
42 CARLTON STREET, E34-440  
CAMBRIDGE, MA 02142

GREG VAN DER VINK  
IRIS  
1200 NEW YORK AVE., NW  
SUITE 800  
WASHINGTON, DC 20005

TERRY WALLACE  
UNIVERSITY OF ARIZONA  
DEPARTMENT OF GEOSCIENCES  
BUILDING #77  
TUCSON, AZ 85721

JAMES WHITCOMB  
NSF  
NSF/ISC OPERATIONS/EAR-785  
4201 WILSON BLVD., ROOM785  
ARLINGTON, VA 22230

JIAKANG XIE  
COLUMBIA UNIVERSITY  
LAMONT DOHERTY EARTH OBSERVATORY  
ROUTE 9W  
PALISADES, NY 10964

OFFICE OF THE SECRETARY OF DEFENSE  
DDR&E  
WASHINGTON, DC 20330

TACTEC  
BATTELLE MEMORIAL INSTITUTE  
505 KING AVENUE  
COLUMBUS, OH 43201 (FINAL REPORT)

PHILLIPS LABORATORY  
ATTN: GPE  
29 RANDOLPH ROAD  
HANSCOM AFB, MA 01731-3010

PHILLIPS LABORATORY  
ATTN: PL/SUL  
3550 ABERDEEN AVE SE  
KIRTLAND, NM 87117-5776 (2 COPIES)

DAVID THOMAS  
ISEE  
29100 AURORA ROAD  
CLEVELAND, OH 44139

LAWRENCE TURNBULL  
ACIS  
DCI/ACIS  
WASHINGTON, DC 20505

FRANK VERNON  
UNIVERSITY OF CALIFORNIA, SAN DIEGO  
SCRIPPS INSTITUTION OF OCEANOGRAPHY IGPP, 0225  
9500 GILMAN DRIVE  
LA JOLLA, CA 92093-0225

DANIEL WEILL  
NSF  
EAR-785  
4201 WILSON BLVD., ROOM 785  
ARLINGTON, VA 22230

RU SHAN WU  
UNIVERSITY OF CALIFORNIA SANTA CRUZ  
EARTH SCIENCES DEPT.  
1156 HIGH STREET  
SANTA CRUZ, CA 95064

JAMES E. ZOLLWEG  
BOISE STATE UNIVERSITY  
GEOSCIENCES DEPT.  
1910 UNIVERSITY DRIVE  
BOISE, ID 83725

DEFENSE TECHNICAL INFORMATION CENTER  
8725 JOHN J. KINGMAN ROAD  
FT BELVOIR, VA 22060-6218 (2 COPIES)

PHILLIPS LABORATORY  
ATTN: XPG  
29 RANDOLPH ROAD  
HANSCOM AFB, MA 01731-3010

PHILLIPS LABORATORY  
ATTN: TSML  
5 WRIGHT STREET  
HANSCOM AFB, MA 01731-3004